İSTANBUL UNIVERSITY PRESS

European Journal of Biology

European Journal of Biology,
EJB 2026, 85 (2): 159–179

https://doi.org/10.26650/EurJBiol.2026.1828061
Submitted: 21.11.2025
Revision Requested: 29.01.2026
Last Revision Received: 16.04.2026
Accepted: 17.04.2026
Published Online 21.05.2026

Research Article

Open Access

Decoding Stress Responses in Barley Lines: Insights Using Next-Generation Sequencing from BOMI and RISO-1508

Esma Ulusoy [1] & Cristina Barrero Sicilia [2]

[1] Uskudar University, Faculty of Engineering and Natural Sciences, Molecular Biology and Genetics, Istanbul, Türkiye
[2] University of Hertfordshire, School of Life and Medical Science, Department of Clinical, Pharmaceutical and Biological Science Center for Agriculture, Hatfield, Hertfordshire, United Kingdom

Abstract

Objective: This study investigated how stress factors (abscisic acid:ABA and heat shock) impact barley genotypes BOMI and its isogenic mutant, RISO-1508, by analyzing gene expression and transcriptomics.

Materials and Methods: The impact of ABA on stress during barley germination was studied, followed by heat shock stress application. After treatment, total RNA was extracted, and cDNA libraries were created for transcriptomic analysis using Oxford Nanopore Technology. Genes with altered expression levels in heat-stressed barley varieties were identified. The most highly expressed DEGs were further examined through GO and KEGG enrichment analyses.

Results: High concentrations of ABA almost completely inhibited barley germination and negatively impacted leaf growth, whereas root growth was less affected. This study is the first to assess the effects of heat stress on BOMI/RISO-1508 cells, revealing significant genetic changes under heat stress. Both genotypes showed similar protective mechanisms by significantly increasing heat shock proteins (HSPs) under heat stress, with BOMI uniquely upregulating five HSPs. A notable difference was observed in fatty acid and energy metabolism, indicating a more robust stress response in the BOMI group. Compared with BOMI, RISO-1508 showed greater downregulation of key photosynthetic genes, such as ATP synthase subunit beta and ribulose biphosphate carboxylase. Under HS, ABA receptor *PYL4-like (LOC123424614)* was significantly increased in BOMI, unlike in RISO-1508, indicating that BOMI has a distinct ABA stress response under HS.

Conclusion: The findings indicate that environmental changes disrupt metabolic pathways in heat stress adaptation due to genotype variations, emphasizing the need to improve heat tolerance in barley.

Keywords *Hordeum vulgare* L. · Barley · BOMI · RISO-1508 · ABA · Heat stress

Citation: Ulusoy, E. & Barrero Sicilia, C. Decoding Stress Responses in Barley Lines: Insights Using Next-Generation Sequencing from BOMI and RISO-1508. Eur J Biol. 2026; 85(2): 159-179. DOI: 10.26650/EurJBiol.2026.1828061

Corresponding author: Esma Ulusoy esma.ulusoy@uskudar.edu.tr

INTRODUCTION

Barley (*Hordeum vulgare* L.) ranks 4th among the most important crops produced in the world. It is a cereal used in industry, especially for malting, brewing, and animal feed.[1] In the brewing industry, barley is mainly produced for malt. Worldwide, 186 million tons of animal feed are produced annually, with 156 million tons used for animal feed and other food industries (FAO, 2022). However, the cultivation area of this valuable agricultural product, with an annual gross value of approximately $45 million, decreased from 73 million hectares in 1994 to 47 million hectares in 2022 and continues to shrink each year.[2] Climate change is the biggest reason for this global challenge, which poses a threat to sustainable crop production as the global population continues to rise.[3,4] Breeding crop varieties that can adapt to changing climatic conditions and stresses, minimize environmental impacts, and increase yields is essential for genetics.[5,6] Many plant varieties, including barley, have been developed for higher yields and resistance to stresses.[7,8] Transgenic crops are often used to improve one or more of these desired traits, and today, transgenic crops, such as corn, rice, and soybean, are permitted for commercial cultivation in many countries.[9] Environmental and genetic changes disrupt crop plants' proteomic and metabolomic pathways.[10,11] Therefore, over the last two decades, transcriptomic studies have proven themselves as a powerful tool in plant science and have helped to reveal the biochemical and genetic factors that affect plant behavior in response to stresses such as drought, salinity, and heat.[12–17]

HSF is crucial for regulating heat shock proteins (HSPs) in all eukaryotes, including plants.[18] HSPs are molecular chaperones that stabilize proteins and membranes and assist in protein refolding during heat stress.[19] Plants have basal thermotolerance, which allows them to withstand temperatures above their optimal growth levels and acquire thermotolerance, thereby enhancing their resistance to extremely high temperatures. Acquired thermotolerance is developed through acclimation to moderately high temperatures, during which a large number of heat-responsive genes, including HSFs and HSPs, are rapidly activated.[16,20–22] Global warming significantly impacts crop yields, necessitating the development of varieties resistant to stress, particularly heat tolerance, which is complex and influenced by genotype-environment interactions.[18,19] Identifying stress-related genes varies among plant varieties[16] and mutants[17], making it essential to find plants with greater heat tolerance.[23] Barley has a greater ability to withstand stress than other cereal crops[14], and its assembled genome sequence has emerged as a model species for studying the genetic and molecular processes of heat tolerance.

Our study focused on two genotypes: BOMI, developed in Denmark in 1969 by crossing the Bonus and Minerva varieties.[24] RISO-1508 is a recessive mutant (lys3a) obtained by treating the BOMI barley variety, the mother line. In the 1970s, Hans Doll and his team at the Risø National Nuclear Laboratory studied around 25 high-lysine barley mutants, leading to the creation of RISO-1508, a chemical-mutagenesis-derived mutant from BOMI.[25] The RISO-1508 barley mutant was developed through ethyl methanesulfonate mutagenesis of the BOMI cultivar. This process induced a recessive mutation in the lys3a gene, located near the centromere region of chromosome 7.[26–29] This mutation resulted in a notable reduction of prolamin levels and an increase in lysine-rich proteins.[30] RISO-1508 also exhibits several notable phenotypic differences compared with its wild-type parent, BOMI. It has shrunken seeds that result in a reduced kernel size and grain yield of 8% and 12%, respectively.[26] In addition, there was a 70% reduction in the prolamin content in RISO-1508, while the lysine content of its proteins increased by 42%.[26] The mutant also shows a 20-30% decrease in starch synthesis and a two-fold increase in sugar content compared to BOMI.[30] There are conflicting reports about the levels of β-amylase in RISO-1508. Moreover, one study indicates that these levels are reduced, whereas another study reports levels that are similar to those of BOMI.[31] The phenotypic alterations emphasize how the lys3a mutation affects the nutritional and agricultural characteristics of RISO-1508 barley compared to wild-type BOMI barley.[32] A feeding trial showed that pigs fed this mutant without protein supplementation experienced a 45% increase in lysine content, similar to milk proteins.[33] RISO-1508 not only supports pig growth but also offers potential benefits for individuals with coeliac disease and the brewing industry due to its lower gluten content.[34]

BPBF is a DNA-binding with one finger (DOF) transcription factor found in barley (*H. vulgare*) and plays a critical role in seed development and germination. During seed development, BPBF supports the provision of adequate nutrient reserves in the endosperm by activating storage protein-encoding genes. Following germination, the action of the BPBF gene stimulates the aleurone layer. This layer regulates genes that regulate hydrolase enzymes, including α-amylase and cathepsin B-like proteases. GAs influence these enzymes by facilitating the activation of nutrients stored in the endosperm. This dual role highlights the crucial function of BPBF in the shift from seed maturation to the germination process.[35]

The expression of BPBF is tightly regulated by plant hormones, being induced by gibberellins (GAs) and repressed by abscisic acid (ABA). Since ABA and GAs act antagonistically in seed biology, the suppression of BPBF by ABA indicates its involvement in ABA-dependent signaling pathways. Consequently, alterations in BPBF gene expression directly influence seed dormancy and germination timing, and may further reflect disruptions in ABA signaling that compromise the plant's capacity to withstand environmental stresses.[36] ABA is a pivotal regulator of plant responses to abiotic stresses, governing both molecular and physiological processes under adverse conditions. Extensive research has demonstrated that ABA-dependent signaling components and stress-responsive gene networks are activated in response to drought, heat, and salinity.[12,13,17,37–39] Beyond stress adaptation, ABA also regulates fundamental developmental processes, including seed maturation, dormancy, germination, and overall plant growth.[38,40–42] Given its central role in abiotic stress regulation, examining differential ABA responses between BOMI and RISO-1508 barley cultivars represents an essential step toward understanding their broader stress tolerance mechanisms. Alterations in ABA signaling can reshape the plant's stress adaptation capacity by modifying the expression of key transcription factors, including *BPBF* and *ABI5*.[43,44] Notably, *ABI5* expression in barley has been shown to play a significant role in ABA-dependent drought responses, further underscoring the importance of intact ABA signaling in mediating effective stress adaptation.[13] Therefore, evaluating the differences in ABA responses of BOMI and RISO-1508 will provide a better understanding of the hormonal regulation involved in stress tolerance in these two cultivars. This basic knowledge will enable a more targeted investigation of these cultivars' broader abiotic stress responses and will contribute to the development of barley cultivars that are more resistant to environmental challenges.

In the final stage of our study, we examined specific genes in relation to transcriptomic data from these two genotypes exposed to short-term heat shock and analyzed differences in response between the barley parent BOMI and the mutant RISO-1508. This study is the first to investigate the effects of heat shock on BOMI-RISO-1508. Figure 1 shows the workflow of the present study.

MATERIALS AND METHODS

Plant Material

Plant Materials and Growth Conditions

H. vulgare, BOMI seeds as a wild-type control, and its mutant line RISO-1508 seeds were obtained from the Life and Medical Science Facilities Centre, University of Hertfordshire. 100 seeds each of BOMI and RISO-1508 were sterilised using 20% sodium hydroxide solution reagent and 3 drops of Tween-20 (Merck, Germany), and then stratified at 4°C in darkness for 4 days to synchronise seed response.[13]

Germination in the Presence of ABA

25 seeds each from wild-type (WT) parent cultivars BOMI and its mutant RISO-1508 were sown in a 9 cm diameter Petri dish (ϕ=90 mm) containing two layers of Whatman filters containing 5 mL of distilled water (control) and ABA solution (75 µM).[13] Seeds were germinated in a growth chamber (22°C, 16 h light/8 h dark). We assessed the germination process by observing root emergence on the 1st, 2nd, 3rd, and 4th days after stratification. The germination test was performed in three biological replicates (each Petri dish containing 25 seeds was considered as one biological replicate). Subsequently, they were observed under a stereoscope for 4 days, and germination percentages were recorded.

Seedling Development in the ABA Presence

The samples were transferred to sterile magentas after 4 days of germination. For ABA treatment in medium, BOMI control/BOMI ABA (50 µM) and RISO-1508 Control/RISO-1508 ABA (50 µM).[13] Seedlings were initially grown on Murashige and Skoog (MS) agar plates and then transferred to MS medium supplemented with or without ABA. MS agar plates were prepared with 3% (w/v) sucrose, 0.7% (w/v) agar, and MS medium adjusted to pH 5.7. Under normal growth conditions, plants were maintained at 22°C in a growth chamber with a photoperiod consisting of 16 h of light followed by 8 h of darkness. After 6 days, the lengths of the first leaf and the longest seminal root of the samples were measured.[13]

Heat-Stress Application

After 10 days of growth (4 days for germination and an additional 6 days for seedling growth), samples from both control BOMI and control RISO-1508 were subjected to heat shock. For the heat stress treatment, half of the BOMI and RISO-1508 samples were transferred to a plant growth cabinet set to a high temperature of 42°C for 3 h.[20,45] The other half was kept in a standard temperature chamber at 22°C for the same duration as the control groups. Heat exposure was conducted in the middle of the day, specifically between 12:00 and 15:00. Three replicate samples, each containing at least 4 seedlings, were used in this experiment. Tissue samples (second leaves) were collected from plants exposed at 42°C and from the control group at 22°C. Three disks were cut from the first shoot leaf of both the heat-shocked and control samples from

each plant, and these disks were stored at -20°C for RNA-Seq analysis.

RNA Purification

RNA was extracted from the second leaves of RISO-1508, and WT plants were collected in three biological replicates. RNA isolation was performed using the E.Z.N.A Plant RNA kit (OMEGA BIO-TEK) for the RNA isolation protocol. The quality of the samples was assessed using agarose gel electrophoresis and Nanodrop. For the RNA-Seq analyses, RNA was additionally purified using the RNeasy Power Clean ProCleanup Kit (QIAGEN) to completely purify the DNA. A NanoDrop (ND-1000) spectrophotometer (NanoDrop Technologies, Wilmington, USA) was used for concentration quantification and quality check.

Preparation of cDNA Libraries and Nanopore Sequencing

After evaluating the quality of pure RNA samples using agarose gel electrophoresis and a Nanodrop spectrophotometer, cDNA was synthesized through polymerase chain reaction (PCR). Next, a cDNA library in three biological replications was prepared for measurement on the MINION device from Oxford Nanopore Technologies (ONT), adhering to the PCR-cDNA sequencing and barcoding protocol (SQK-PCB109). All assays were conducted for sequencing at the University of Hertfordshire. For cDNA synthesis, we used the direct cDNA sequencing-native barcoding kit (SQK-DCS109). A ~50 ng of total RNA was amplified in a 20 µL reaction volume using a BIO-RAD PCR System. The initial step involved incubation at 42°C for 2 min after adding 1 µL of Maxima H Minus Reverse Transcriptase. The reaction conditions consisted of reverse transcription and strand-switching at 42°C for 90 min (1 cycle) followed by 5 min at 85°C (1 cycle). In the subsequent PCR step, barcodes were added to each cDNA sample using Barcode Primers (BP01-BP12). The initial denaturation occurred at 95°C for 30 sec, followed by 15 cycles of 95°C for 15 sec, annealing at 62°C for 15 sec, and extension at 65°C for 150 sec, concluding with a final extension at 65°C for 6 min. We applied 1 µL of NEB exonuclease for end repair, followed by adapter ligation. After amplifying the cDNA, we measured its concentration using a Qubit fluorometer (Invitrogen Life Technologies, USA). The cDNA Nanopore libraries were then loaded onto a Flow Cell (FLO-MIN106) and sequenced using the MinION Mk1B. The raw reads were base-calling using MinKNOW with default parameters for the following sequencing. Data preprocessing was conducted using the Galaxy Europe Program.

Processing and Analysis of Long-Read Oxford Nanopores

All MinION FASTQ files were transferred to Galaxy Prog. Each barcode has multiple FASTQ files, which we merged using the concatenate datasets tool. We performed adapter trimming with the Porechop adapter trimmer for ON reads (Galaxy Version 0.2.4+galaxy0). The data quality was then assessed using the NanoPlot plotting suite for ON sequencing data and alignments (Galaxy Version 1.43.0+galaxy0). Full-length read data were combined with a gene feature file to obtain the feature counts. These were then mapped to the reference genome of *H. vulgare* L. and the annotation (NCBI-RefSeq) GCF_904849725.1–MorexV3_pseudomolecules_assembly using minimap2 (Galaxy Version 2.28+galaxy0). After mapping, the quality of all 12 barcodes was assessed using the feature count summary files, which compile results from bioinformatics analyses into a single report generated by the tool MultiQC (Galaxy Version 1.24.1+galaxy0). The uniquely mapped reads were used to identify differentially expressed genes (DEGs). After this preparation, we analysed the treated (heat) and untreated (no heat) groups, generating the final heatmap, Heatmap2, using the z-scores from the differential expression analysis tool, DESeq2. This tool identifies differentially expressed features from count tables (Galaxy Version 2.11.40.8+galaxy0). Data from BOMI control (BC) and BOMI heat (BH), as well as RISO-1508 control (RC) and RISO-1508 heat (RH), were analysed in pairs through gene-level differential expression analyses for the two conditions. We filtered the final outputs for q-value ≤0.05 and log2 (Fold Change, FD) ≥0.5, and visualised the gene IDs along with the descriptions of the up- and downregulated genes associated with both BC/BH and RC/RH. We also visualized the upregulated and downregulated genes for BC/BH and RC/RH using the Volcano Plot tool (Galaxy Version 0.0.6). In addition, we represented the numbers of upregulated and downregulated genes in a Venn diagram created from the lists generated by DESeq2 (Galaxy Version 0.1.1).

Gene Ontology Enrichment Analysis of Differentially Expressed Genes

Functional enrichment analysis of the common DEGs was performed using the DAVID Knowledgebase (v2023q4) via the DAVID 2021 (Dec. 2021) platform.[46] This high-throughput tool was utilized to categorize DEGs from the leaf tissues of BOMI and RISO-1508 under heat stress into three GO domains: BP, CC, and MF. Kyoto Encyclopedia of Genes and Genomes (KEGG) pathway analysis was employed to map molecular interactions and associations within specific biological pathways.[47] An EASE threshold (p-value) of <0.01

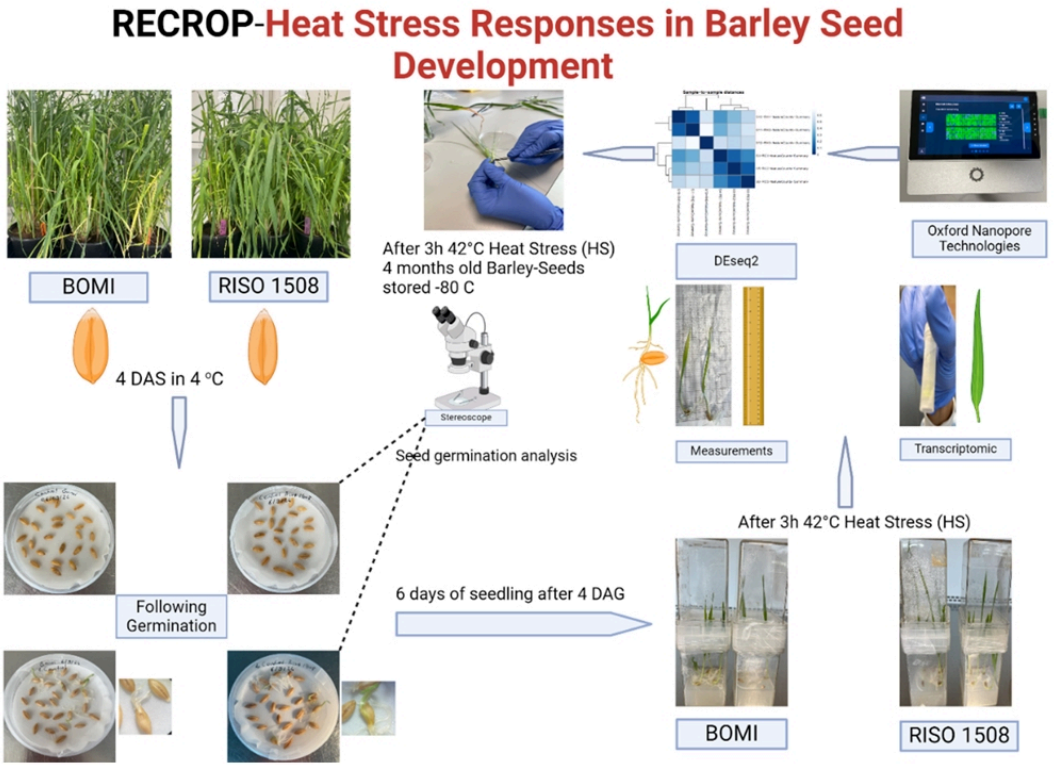

Figure 1. The project, prepared under the RECROP COST Action, summarizes the experimental workflow for heat stress responses in barley seed development: Two barley genotypes (BOMI and RISO-1508 1508) were germinated at 4°C and subjected to heat stress (42°C, 3h). Seed germination and early seedling development were assessed by stereoscopy at 4 days of stratification and 6 days of germination. Following heat stress treatment, phenotypic measurements and transcriptomic analyses were performed. Gene expression data obtained via Oxford Nanopore Technologies were processed using DESeq2 to identify differentially expressed genes between genotypes under heat stress conditions.

and a minimum count of 3 defined the criteria for statistical significance. The final analysis performed the results from both the Functional Annotation Chart and Functional Annotation Clustering modules to identify the most biologically relevant gene groups. Transcripts with a log2 (FC) of ≥0.5 were considered as differentially expressed transcripts. Unsupervised hierarchical clustering of differentially expressed genes was performed using Cluster, and the results were visualized using GraphPad Prism 11. Figure 1 shows the workflow of the present study.

RESULTS

Seed Germination

In the first phase of our work, we investigated the responses of BOMI and RISO-1508 to ABA during seed germination after 4 days of stratification. The germination dynamics of the RISO-1508 mutant and its WT, BOMI, showed no differences under control conditions (Figure 2). However, after treatment with 75 µM ABA, both BOMI and RISO-1508 seeds exhibited nearly complete inhibition of germination.

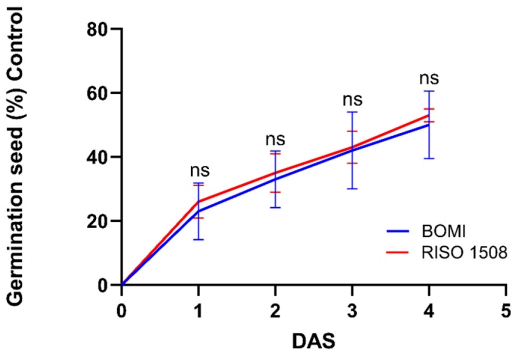

Figure 2. Germination of RISO-1508 and BOMI seeds Multiple unpaired t-tests of BOMI&RISO-1508 seed germination percentage were performed. No significant (ns) differences were observed between these barley varieties.

RISO-1508 Sensitivity to ABA at the Seedling Development Stage

Following these results, we transferred the 4-day-old germinated control seeds and analysed the development of 6-day-old seedlings in the presence of 50 µM ABA. We found that ABA negatively affected the growth of the first leaf

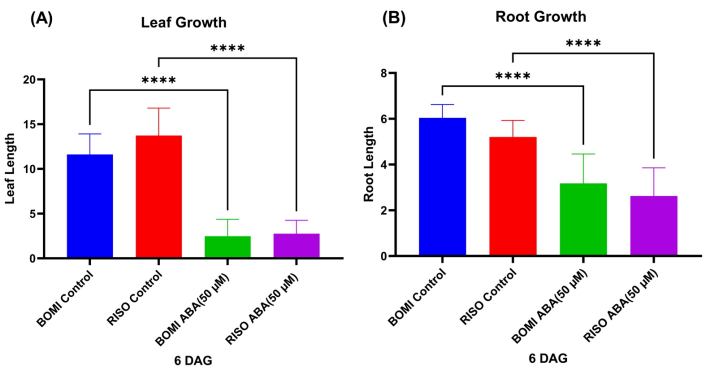

Figure 3. (**A**) Growth of the first leaf of analysed seedlings after 6 d of ABA treatment. (**B**) Growth of the longest seminal root of seedlings after 6 days of ABA treatment. **** p<0.0001

in both lines, but there were no significant differences in leaf length (Figure 3A) or the length of the longest seminal root (Figure 3B) between these genotypes, regardless of ABA exposure. However, we observed significant differences in ABA-dependent inhibition between RISO-1508 and BOMI, relative to their respective control conditions (Figure 3A and 3B). In addition, both RISO-1508 and BOMI exhibited considerably lower ABA-dependent root inhibition than their respective control groups (Figure 3B).

RNA Sequencing and Data Processing

Total RNA was isolated from the second leaves of 10-day-old seedlings and used for direct RNA sequencing with the MinION. RNA sequencing reads were analysed using the Galaxy programme, minimap2, and featureCounts for MultiQC (Galaxy Version 1.24.1+galaxy0) quality checking**.** The observed mapping rates (>50%) are consistent with ONT long-read sequencing benchmarks for plant transcriptomes using PCR-cDNA protocols. The reduced mapping efficiency compared with short-read platforms reflects the characteristic ONT base-calling error rates and the repetitive architecture of the *H. vulgare* genome (Morex v3), rather than sample quality deficiencies. The reads were mapped to the artificially created genome sequence by DESeq2. The mapped DESeq2 reads used for the heat map were used for further analysis.

Transcriptome Analysis of BOMI and RISO-1508 under Heat Stress

In the second phase of our study, we conducted transcriptomic analysis, enabling us to examine gene activity in response to these conditions. The effects of short-term heat shock on two genotypes were investigated, with BOMI as a wild-type control and RISO-1508 as its mutated line. The heat stress treatment included exposing the samples to 42°C for 3 h. RNA sequencing data were collected, and DEGs were identified using DESeq2. The up- and downregulated genes were presented with a heatmap, a z-score plot, and a volcano plot, and the overlapping genes were illustrated using a Venn diagram. This study is unique in that it is the first to investigate the effects of BOMI-RISO-1508 on heat shock. Transcriptomic analyses revealed significant genetic changes in BOMI and RISO-1508 under heat stress conditions. The acceptability of the total RNA sequencing data (>50% match) supports our findings. DESeq2 analysis indicates that BOMI and RISO-1508 respond to heat stress in distinct and shared ways: Heatmap and z-score plots are matrices showing gene expression levels and are powerful tools for visualising the results. In this study, the barley genotypes BOMI and RISO-1508 were used to investigate their responses to heat shock. Samples were prepared in triplicate as BC (BOMI Control), BH (BOMI Heat Shock), RC (RISO-1508 Control), and RH (RISO-1508 Heat Shock), making the differences in gene expression visible at a glance. In the heatmap, red and lighter tones represent high expression and low or near-control expression, respectively. The Z-score map is a heatmap showing how much the expression of each gene deviates from the mean across samples. Red indicates the above (upregulated) and blue indicates the below (downregulated) expression. This allows for a clearer assessment of variations in gene expression and responses to heat stress conditions.

BOMI Genotype Response to Heat Stress (BOMI heatmap and BOMI Z-score)

Significant changes in gene expression were observed in the BOMI genotype after heat stress was applied.

Upregulation of HSPs and Similar Genes

In the BOMI heatmap, the gene ID and genes are described (Figure 4A). Genes coding for heat shock proteins, such as 70 kDa heat shock protein, 16.9 kDa class I heat shock protein 1-like, 26.2 kDa heat shock protein, mitochondria, and small heat shock protein, are significantly upregulated (dark red colour) in cells under heat shock (BH samples).

Downregulation of Photosynthetic and Ribosomal Genes.

In the Z-score map of BOMI Gene IDs and the description (Figure 4B), some genes coding for maturase K, chaperone protein ClpB2, chloroplastic, NAD(P)H-quinone oxidoreductase subunit, and 30S ribosomal protein S7, chloroplastic, were downregulated (blue colour) in the BOMI heat shock samples.

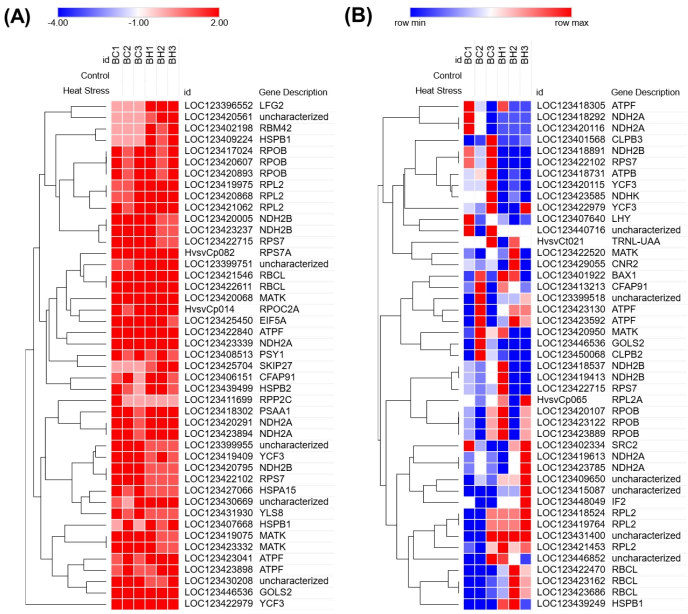

Figure 4. (A) BOMI gene IDs are classified according to expression intensity. DESeq2 data from BOMI control (BC) and BOMI heat (BH) were analysed for gene-level differential expression. Gene IDs, descriptions, and related intensity genes for BC and BH are presented. **(B)** BOMI gene IDs are filtered for final outputs using a q-value of ≤0.05 and a log2 (FC) of ≥0.5, visualising the gene IDs with descriptions of up- and downregulated genes related to BC/BH. Red indicates upregulation, blue indicates downregulation. BOMI gene IDs are shown with descriptions of genes associated with BC and BH.

RISO-1508 Genotype Response to Heat Stress (RISO-1508 Heatmap and RISO-1508 Z-score)

Similar changes in gene expression were observed in the RISO-1508 genotype under heat shock.

Upregulation of HSPs and Similar Genes

The heatmap for RISO-1508 shows gene IDs and their corresponding gene names (Figure 5A), which are related to HS proteins. Specifically, proteins such as heat shock protein 70 kDa, heat shock cognate 70 kDa protein 2, 26.2 kDa heat shock protein, mitochondrial, and 16.9 kDa class I heat shock protein

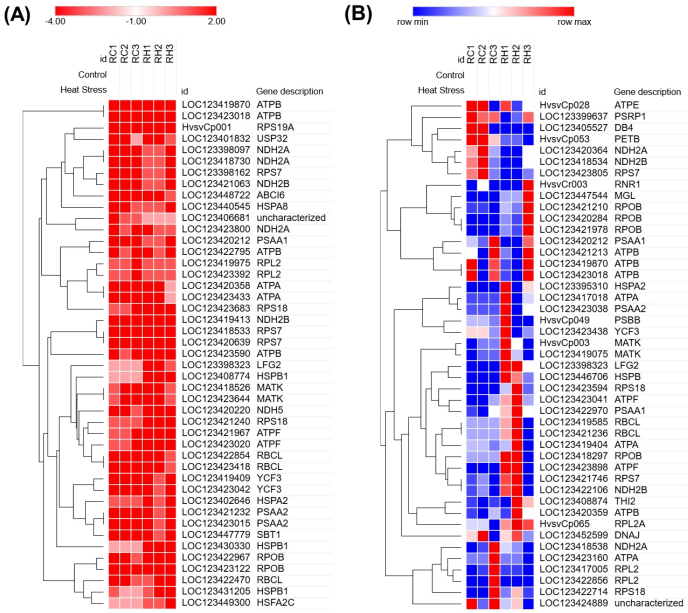

Figure 5. (A) RISO-1508 gene IDs are classified by expression levels based on DESeq2 analysis from RISO-1508 control (RC) and heat (RH), showing descriptions and related intensity genes. **(B)** Filtered for q-value ≤0.05 and log2(FC) ≥0.5, gene IDs are displayed with descriptions of up- and downregulated genes in RC and RH, with red and blue indicating up- and downregulation, respectively.

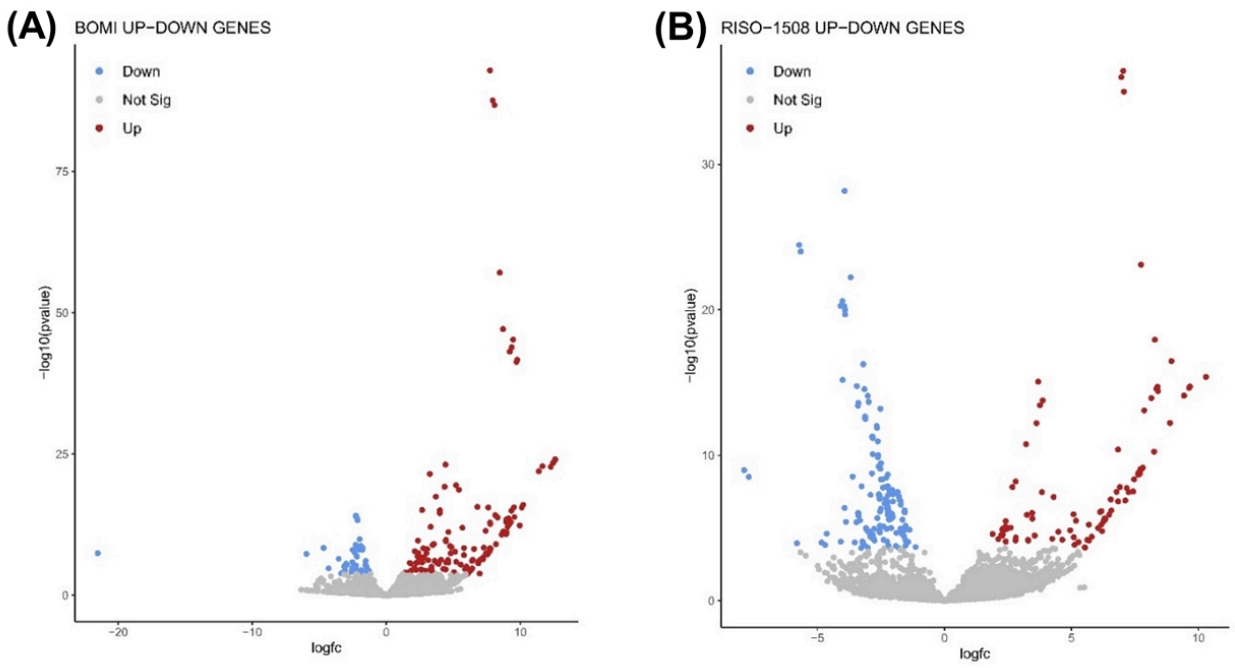

Figure 6. (A) The BOMI gene plot visualizes both upregulated and downregulated genes using a volcano plot for BC/BH. **(B)** The RISO-1508 gene plot visualizes both up- and downregulated genes using a volcano plot for RC/RH.

1-like were upregulated (represented in red) in the heat shock samples from RISO-1508 (RH samples).

Significant Downregulation of Photosynthetic and Ribosomal Gene Expression

Gene IDs are identified in the RISO-1508 z-score map, and the corresponding genes are described in Figure 5B. Many genes, particularly those located in the upper part of the map (such as ATP synthase subunit beta, chloroplastic, photosystem I assembly protein Ycf3, and 30S ribosomal protein S7, chloroplastic), are significantly downregulated (indicated by blue colour) under heat shock conditions. Additionally, photosynthesis-related genes, including the gene coding ribulose bisphosphate carboxylase, are downregulated. The results of the heat maps were examined, it was observed that genes coding proteins related to photosynthesis, such as ribulose biphosphate carboxylase, photosystem I, and NAD(P)H-quinone oxidoreductase, were downregulated under heat stress in BOMI and RISO-1508, whereas genes coding 16.9 kDa class 1 heat shock protein and heat shock protein 70 kDa were significantly upregulated under heat stress. Both genotypes showed similar primary responses in upregulating HSPs in response to heat. However, the z-score maps show that the downregulation of photosynthetic and ribosomal genes, particularly in RISO-1508, may be more widespread and significant compared with that in BOMI.

Volcano Plot Analysis

Volcano plots for BOMI (Figure 6A) and RISO-1508 (Figure 6B) show the distribution and statistical significance of the differentially expressed genes. These plots visualize whether genes are upregulated or downregulated based on their log2 (FC) values and p-values. The volcano plots provide a qualitative overview of the differential gene expression profiles between BOMI and RISO-1508 in response to heat stress. The BOMI plot reveals a broader distribution of genes exhibiting higher log2 (FC) values and lower p-values, indicating a more robust and extensive heat stress transcriptional response. Key upregulated genes in BOMI, such as *HSP26.2-Mit*, *HSP17.5-CII*, *HSP21.9*, *HSP23.2*, and *ClpB1*, underscore a vigorous chaperone-mediated stress response. Here, they appear to respond similarly to heat shock genes without *HSP16.9-CI-1,* but the response of BOMI is quantitatively greater, as seen from the log2 (FC) values. In contrast, the RISO-1508 volcano plot displayed a narrower distribution, indicating that fewer genes achieved significant fold change values. Notably, RISO-1508 significantly downregulated critical photosynthetic genes, including the RuBisCO large subunit, ATP synthase beta subunit, and various chlorophyll a/b binding proteins, indicating a significant disruption in photosynthetic capacity**.** These findings are presented in Tables 1 and 2 , which list the top 10 most significant up/down DEGs for BOMI and RISO-1508.

Table 1. Top 10 upregulated and downregulated differentially expressed genes (DEGs) in patients with BOMI.

Gene ID	Gene Name (Abbreviation)	Log_2(FC)	Gene ID	Gene Name (Abbreviation)	Log_2(FC)
	▲ Upregulated			▼ Downregulated	
LOC123409224	*HSP26.2-Mit*	9.96E+14	HvsvCt003	*trnK (tRNA-Lys)*	−5.95E+14
LOC123439502	*HSP17.5-CII*	9.76E+14	LOC123418526	*matK*	−4.67E+14
LOC123439504	*HSP17.5-CII*	9.71E+14	LOC123418804	*matK*	−4.67E+14
LOC123451172	*HSP21.9*	9.55E+14	LOC123419075	*matK*	−4.67E+14
LOC123426475	*PPIL-70*	9.52E+14	LOC123420000	*matK*	−4.67E+14
LOC123439500	*HSP17.5-CII*	9.46E+14	LOC123420871	*matK*	−4.67E+14
LOC123439499	*HSP17.5-CII*	9.36E+14	LOC123420950	*matK*	−4.67E+14
LOC123430330	*HSP23.2*	9.34E+14	LOC123421497	*matK*	−4.67E+14
LOC123446999	*ClpB1*	9.29E+14	LOC123421741	*matK*	−4.67E+14
LOC123439501	*HSP17.5-CII*	9.20E+14	LOC123421982	*matK*	−4.67E+14

Abbreviations: FC: Fold Change; HSP, heat shock protein; Mit, mitochondrial; Chl, chloroplastic; CI/CII, class I/class II; matK, maturase K; trnK/trnL, transfer RNA genes; rps3, ribosomal protein S3; TST16, thiosulfate sulfurtransferase 16; CIP8, E3 ubiquitin-protein ligase; LFG2, LIFEGUARD 2; ClpB1, chaperone protein ClpB1; BAG6, BAG family molecular chaperone regulator 6; DREB1B, dehydration-responsive element-binding protein 1B; SERF2, small EDRK-rich factor 2. Gene names are abbreviated following the standard nomenclature (HGNC/plant gene nomenclature guidelines). Italic font indicates gene/protein abbreviations.

Table 2. Top 10 differentially expressed genes (DEGs) upregulated and downregulated in RISO-1508.

Gene ID	Gene Name (Abbreviation)	Log_2(FC)	Gene ID	Gene Name (Abbreviation)	Log_2(FC)
	▲ Upregulated			▼ Downregulated	
LOC123439502	*HSP17.5-CII*	9.66E+14	HvsvCt003	*trnK (tRNA-Lys)*	−7.89E+14
LOC123439504	*HSP17.5-CII*	9.63E+14	HvsvCt021	*trnL (tRNA-Leu)*	−7.70E+14
LOC123439501	*HSP17.5-CII*	9.43E+14	LOC123396665	*DREB1B*	−5.81E+14
LOC123439252	*HSP16.9-CI-1*	8.88E+14	HvsvCp003	*matK*	−5.72E+14
LOC123439249	*HSP16.9-CI-1*	8.39E+14	LOC123406681	*uncharacterised*	−5.67E+14
LOC123442568	*HSP16.9-CI-1*	8.34E+14	LOC123418526	*matK*	−5.66E+14
LOC123442570	*HSP16.9-CI-1*	8.15E+14	LOC123418804	*matK*	−5.66E+14
LOC123431205	*HSP16.9-CI-1*	7.87E+14	LOC123419075	*matK*	−5.66E+14
LOC123412813	*HSP26.2-Mit*	7.81E+14	LOC123420000	*matK*	−5.66E+14
LOC123446664	*HSP17.9-CI*	7.74E+14	LOC123420871	*matK*	−5.66E+14

Abbreviations: FC: Fold change; HSP, heat shock protein; Mit, mitochondrial; Chl, chloroplastic; CI/CII, class I/class II; matK, maturase K; trnK/trnL, transfer RNA genes; rps3, ribosomal protein S3; TST16, thiosulfate sulfurtransferase 16; CIP8, E3 ubiquitin-protein ligase; LFG2, LIFEGUARD 2; ClpB1, chaperone protein ClpB1; BAG6, BAG family molecular chaperone regulator 6; DREB1B, dehydration-responsive element-binding protein 1B; SERF2, small EDRK-rich factor 2. Gene names are abbreviated following the standard nomenclature (HGNC/plant gene nomenclature guidelines). Italic font indicates gene/protein abbreviations.

Identification of Heat Stress-Regulated Genes in the BOMI and RISO-1508 Groups using a Venn Diagram

185 upregulated genes were identified in the BOMI group and 126 in the RISO-1508 group. Ninety genes were upregulated in both groups (Figure 7A). However, 262 and 452 downregulated genes were identified in the BOMI group and 452 in the RISO-1508 group. 251 of these genes were downregulated in both groups (Figure 7B).

GO Analysis of the DEGs

Functional and pathway enrichment analyses of common DEGs were conducted using DAVID software. The upregulated DEGs for BOMI and RISO-1508 yielded 3 clusters ($p<0.01$,

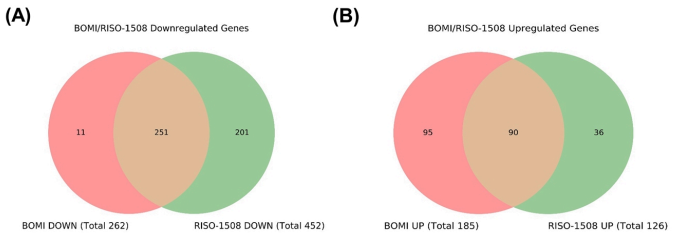

Figure 7. (A) The number of downregulated genes for BOMI and RISO-1508, derived from DESeq2 lists, is shown in the Venn diagram. This study highlights shared and unique downregulated genes influenced by BOMI and RISO-1508 under heat stress. **(B)** Similarly, the Venn diagram shows the number of upregulated genes associated with BOMI and RISO-1508 based on lists generated by DESeq2. This study illustrates the shared and unique upregulated genes affected by BOMI and RISO-1508 in response to heat stress.

Table 3. Gene Ontology (GO) analysis of differentially expressed genes (DEGs) in upregulated BOMI.

Category	Pathway	Genes %	Count	P-value
Biological Process	Response to the heat	19%	35	5.29E-56
	Protein complex oligomerization	11%	20	6.14E-40
	Protein folding	16%	30	3.94E-38
	Response to hydrogen peroxide	11%	20	3.64E-32
	Response to the salt stress	11%	20	1.34E-24
	Protein refolding	8%	15	9.93E-20
	Cellular response to unfolded protein	6%	11	3.21E-17
	Cellular Response to Heat	6%	12	2.53E-14
	Response to the virus	3%	6	3.61E-09
	Response to Stress	6%	12	9.86E-08
	Protein stabilisation	2%	3	6.41E-03
Cellular Component	Cytoplasm	28%	51	1.16E-14
	The perinuclear region of the cytoplasm	2%	3	2.01E-03
	Protein-containing complex	2%	3	3.07E-03
Molecular Function	Unfolded protein binding	20%	37	4.44E-57
	ATP-dependent protein folding	8%	15	2.15E-20
	Misfolded protein binding	6%	11	2.81E-17
	Heat shock protein binding	6%	11	2.92E-16
	Protein-Folding Chaperone	6%	11	4.36E-14
	ATP hydrolysis activity	10%	19	1.12E-10
	Protein-folding chaperone binding	4%	8	1.01E-09
	RNA Polymerase II	4%	7	4.90E-04
	Oxidoreductase activity	2%	3	5.64E-04
	Activity of adenyl-nucleotide exchange factor	2%	3	2.34E-03
	Hsp70 binding	2%	3	2.34E-03

P-values were calculated using the DAVID functional annotation tool. Only terms with P<0.05 are shown.

enrichment score 2.47-38.58) and 4 clusters (p<0.01, enrichment score 2.67-45.34), respectively, with enrichment across the "molecular function," "biological process," and "cellular component" categories. Tables 3 and 4 provide the GO terms for the upregulated genes of BOMI and RISO-1508. The downregulated DEGs for BOMI and RISO-1508 identified 8 clusters (p<0.01, enrichment score 11.88-94.67) and 9 clusters (p<0.01, enrichment score 22.89-141.08), respectively. The GO terms for these genes are listed in Tables 5 (BOMI) and 6 (RISO-1508).

GO Enrichment of Upregulated and Downregulated DEGs

Upregulated DEGs in both genotypes converged on molecular chaperone and proteostasis pathways, yet exhibited genotype-specific differences in the mode of protein quality control. In BOMI, response to heat (19%, n=35, $P=5.29\times10^{-56}$), protein folding (16%, n=30, $P=3.94\times10^{-38}$), and protein refolding ($P=9.93\times10^{-20}$) were the dominant BP terms, with MF enrichment centred on unfolded protein binding (20%, n=37, $P=4.44\times10^{-57}$) and ATP-dependent protein folding chaperone ($P=2.15\times10^{-20}$) (Table 3), consistent with a chaperone-driven refolding strategy. In RISO-1508, while response to heat (25%, n=32, $P=3.61\times10^{-52}$) and protein folding ($P=5.28\times10^{-35}$) were similarly enriched, the genotype-specific terms modification-dependent protein catabolic process ($P=5.09\times10^{-17}$), protein ubiquitination ($P=2.56\times10^{-7}$), protein tag activity ($P=3.81\times10^{-17}$), and ubiquitin protein ligase binding ($P=9.99\times10^{-17}$) were exclusively enriched (Table 4), indicating a shift towards ubiquitin-proteasome system (UPS)-mediated protein degradation rather than chaperone-assisted refolding.

Downregulated DEGs were predominantly associated with photosynthetic and chloroplast functions in both genotypes. However, the extent and severity of suppression differed markedly between BOMI and RISO-1508. In BOMI, the most significantly enriched BP terms included carbon fixation (10%, n=27, $P=7.11\times10^{-44}$), reductive pentose-phosphate

Table 4. GO analysis of differentially expressed genes (DEGs) in RISO-1508 – Upregulated.

Category	Pathway	Genes %	Count	P-value
Biological Process	Response to the heat	25%	32	3.61E-52
	Protein complex oligomerization	16%	20	1.75E-41
	Protein folding	21%	27	5.28E-35
	Response to hydrogen peroxide	16%	20	1.06E-33
	Response to the salt stress	16%	20	4.10E-26
	Modification-dependent catabolic process of proteins	10%	13	5.09E-17
	Cellular response to unfolded protein	7%	9	1.11E-13
	Protein refolding	9%	11	1.39E-13
	Cellular Response to Heat	7%	9	3.54E-10
	Response to the virus	5%	6	1.53E-09
	Response to Stress	10%	12	1.66E-08
	Protein ubiquitination	13%	16	2.56E-07
	Protein stabilisation	2%	3	4.62E-03
	The polyketide biosynthetic process	2%	3	5.83E-03
Cellular Component	Cytoplasm	44%	56	7.09E-26
	The perinuclear region of the cytoplasm	2%	3	1.19E-03
	Protein-containing complex	2%	3	1.82E-03
Molecular Function	Unfolded protein binding	28%	35	2.30E-55
	Protein tag activity	10%	13	3.81E-17
	Ubiquitin-binding protein ligase	10%	13	9.99E-17
	ATP-dependent protein folding	10%	12	1.04E-15
	Misfolded protein binding	7%	9	1.18E-13
	Heat shock protein binding	7%	9	7.14E-13
	Protein-Folding Chaperone	7%	9	3.51E-11
	ATP hydrolysis activity	13%	16	7.42E-09
	Messenger RNA (mRNA) binding	11%	14	5.55E-07
	Protein-folding chaperone binding	5%	6	7.81E-07
	Hsp70 binding	2%	3	1.78E-03

P-values were calculated using the DAVID functional annotation tool. Only terms with P<0.05 are shown.

cycle (11%, n=28, $P=6.96\times10^{-42}$), and photorespiration ($P=6.56\times10^{-40}$), alongside suppression of proton motive force-driven ATP synthesis ($P=3.27\times10^{-29}$) and ribosomal small subunit assembly ($P=6.83\times10^{-36}$) (Table 5). CC enrichment confirmed large-scale dismantling of chloroplast (45%, n=118, $P=4.04\times10^{-94}$) and thylakoid membrane components ($P=2.71\times10^{-36}$). In RISO-1508, suppression was far broader and more statistically extreme: proton transmembrane transport (17%, n=75, $P=2.12\times10^{-81}$), mitochondrial ATP synthesis ($P=3.46\times10^{-67}$), and photosynthesis (14%, n=65, $P=3.26\times10^{-61}$) were among the top enriched terms (Table 6). In RISO-1508, ATP synthase activity, rotational mechanism (18%, n=80, $P=1.26\times10^{-118}$), chlorophyll binding ($P=9.14\times10^{-41}$), and electron transfer activity ($P=9.39\times10^{-26}$) were significantly enriched, indicating a more comprehensive collapse of both photosynthetic and mitochondrial electron transport chains in the heat-sensitive genotype.

KEGG Pathway Analysis of DEGs

KEGG pathway analyses revealed that downregulated genes were significantly enriched in seven pathways, including mitochondrial energy metabolism and photosynthesis, with a notable decline in secondary metabolite biosynthesis in BOMI. In contrast, upregulated genes were enriched in three pathways, particularly "Protein processing in the ER" BOMI showed higher energy metabolism activation than RISO-1508, while RISO-1508 had greater activity in the hormone-related pathway "Ubiquitin-mediated proteolysis" compared to BOMI (Table 7).

Table 5. Gene Ontology (GO) analysis of differentially expressed genes (DEGs) in Downregulated BOMI.

Category	Pathway	Genes %	Count	P-value
Biological Process	Carbon fixation	10%	27	7.11E-44
	Reductive pentose-phosphate cycle	11%	28	6.96E-42
	Photorespiration	11%	28	6.56E-40
	Ribosomal assembly of small subunits	10%	26	6.83E-36
	tRNA processing	10%	25	1.94E-33
	Cytoplasmic translation	10%	25	2.81E-31
	Proton Motive Force-Driven ATP Synthesis	10%	26	3.27E-29
	DNA-templated transcription	11%	30	1.74E-26
	RNA splicing	10%	25	1.46E-25
	ATP synthesis coupled with electron transport	8%	21	3.28E-24
	Photosynthesis and light reaction	8%	21	5.24E-21
	Translation	13%	34	5.05E-19
	Messenger RNA (mRNA) processing	10%	25	1.61E-17
	Photosynthesis	9%	23	2.92E-16
Cellular Component	Chloroplast	45%	118	4.04E-94
	Ribosome	21%	56	4.41E-44
	The DNA-directed RNA polymerase complex	11%	29	1.42E-38
	Large ribosomal subunit	10%	27	7.62E-37
	SRS subunit	11%	28	1.77E-36
	The chloroplast thylakoid membrane	19%	50	2.71E-36
	Proton-transporting ATP synthase complex	11%	28	4.00E-26
	Plastid	9%	24	7.08E-26
Molecular Function	Structural constituents of the ribosomes	23%	60	3.55E-50
	Activity of ribulose-bisphosphate carboxylase	11%	28	1.85E-46
	Proton transmembrane transporter activity	10%	25	1.86E-38
	rRNA binding	13%	33	2.02E-36
	DNA-Directed RNA Polymerase Activity	11%	30	2.45E-34
	Quinone binding	8%	22	1.46E-28
	NADH dehydrogenase (ubiquinone) activity	8%	22	5.19E-24
	Magnesium ion binding	11%	29	4.91E-23
	Transferase activity	10%	27	1.87E-22
	RNA binding	19%	51	3.44E-22
	Monooxygenase activity	11%	28	8.81E-15
	Messenger RNA (mRNA) binding	9%	24	2.90E-08
	ATP synthase activity and rotational mechanism	2%	6	3.39E-03
	DNA binding	11%	30	3.77E-03

P-values were calculated using the DAVID functional annotation tool. Only terms with P<0.05 are shown.

KEGG Enrichment of Upregulated and Downregulated DEGs

KEGG pathway analysis corroborated the GO findings and further highlighted disproportionate metabolic disruption in RISO-1508 compared with that in BOMI (Table 7). Among the upregulated DEGs, protein processing in the ER was the most significantly enriched pathway in both genotypes—BOMI (26%, n=49, $P=1.59\times10^{-68}$) and RISO-1508 (37%, n=47, $P=5.53\times10^{-72}$)—confirming that ER-associated protein quality control is a conserved heat stress response in barley (Table 7). The spliceosome and endocytosis pathways were enriched in both genotypes, indicating shared post-transcriptional regulatory and membrane trafficking responses. Ubiquitin-mediated

Table 6. GO analysis of differentially expressed genes (DEGs) in RISO-1508 – Downregulated.

Category	Pathway	Genes %	Count	P-value
Biological Process	Proton transmembrane transport	17%	75	2.12E-81
	Proton Motive Force-Driven ATP Synthesis	12%	54	1.19E-69
	Mitochondrial ATP synthesis	10%	47	3.46E-67
	Photosynthesis	14%	65	3.26E-61
	Carbon fixation	6%	27	3.15E-37
	Translation	14%	62	1.10E-35
	Reductive pentose-phosphate cycle	6%	28	5.34E-35
	Photorespiration	6%	28	4.79E-33
	ATP synthesis coupled with electron transport	6%	28	9.61E-30
	Ribosomal assembly of small subunits	6%	26	1.42E-29
	Cytoplasmic translation	6%	25	2.83E-25
	DNA-templated transcription	8%	34	6.90E-24
	Photosynthesis and light reaction	6%	25	3.57E-21
	tRNA processing	4%	18	9.42E-17
	RNA splicing	4%	18	1.01E-11
	Messenger RNA (mRNA) processing	4%	18	1.05E-06
	Electron transport coupled with proton transport	2%	7	2.90E-05
	Aerobic respiration	2%	7	2.39E-03
Cellular Component	The chloroplast thylakoid membrane	37%	166	4.92E-182
	Proton-transporting ATP synthase complex	23%	102	5.01E-144
	Chloroplast	39%	178	3.60E-129
	Thylakoid	15%	68	4.58E-88
	Plastid thylakoid membrane	10%	45	5.05E-71
	Ribosome	18%	80	2.37E-56
	Photosystem I	8%	38	1.53E-42
	The DNA-directed RNA polymerase complex	7%	33	2.67E-38
	Large ribosomal subunit	6%	29	9.02E-34
	Mitochondrial small ribosomal subunit protein	6%	27	1.93E-33
	SRS subunit	7%	30	5.45E-33
	Plastid	5%	24	2.61E-20
	Mitochondrion	11%	49	1.08E-15
	Ribonucleoprotein complex	7%	31	1.38E-15
Molecular Function	ATP synthase activity and rotational mechanism	18%	80	1.26E-118
	rRNA binding	13%	59	1.35E-68
	Structural constituents of the ribosomes	19%	87	3.22E-66
	Magnesium ion binding	14%	65	2.46E-60
	Chlorophyll binding	9%	41	9.14E-41
	Activity of ribulose-bisphosphate carboxylase	6%	28	1.09E-39
	4 iron, 4 sulfur cluster binding	9%	39	5.61E-39
	DNA-Directed RNA Polymerase Activity	8%	34	6.69E-33
	Proton transmembrane transporter activity	6%	25	1.70E-32
	Small ribosomal subunit rRNA binding	5%	24	1.40E-31
	NADH dehydrogenase (ubiquinone) activity	7%	30	3.16E-30
	Quinone binding	5%	24	1.23E-26
	Electron transfer activity (ETA)	9%	39	9.39E-26
	ATP hydrolysis activity	10%	47	4.95E-18
	Transferase activity	6%	27	1.95E-16
	Oxidoreductase activity	8%	38	4.24E-11
	Monooxygenase activity	6%	29	8.02E-10
	ADP binding	6%	29	9.48E-09
	RNA binding	10%	44	2.02E-08
	Messenger RNA (mRNA) binding	6%	25	1.11E-04
	ATP binding	17%	77	5.32E-04

P-values were calculated using the DAVID functional annotation tool. Only terms with P<0.05 are shown.

Table 7. KEGG pathway analysis of common DEGs in BOMI and RISO-1508 cells

DEG Group	KEGG Pathway	Genes %	Count	P-value
Downregulated BOMI	Oxidative phosphorylation	31%	80	6.49E-82
	Metabolic pathways	42%	111	1.21E-39
	Glyoxylate and dicarboxylate metabolism	11%	29	4.88E-34
	RNA polymerase	11%	30	3.05E-33
	Carbon fixation by the Calvin cycle	11%	28	1.03E-31
	Photosynthesis	13%	33	4.61E-25
	Carbon metabolism	11%	29	9.13E-21
	Biosynthesis of secondary metabolites	11%	29	3.07E-03
RISO-1508 – Downregulated	Oxidative phosphorylation	38%	171	5.61E-198
	Photosynthesis	33%	149	3.57E-191
	Metabolic pathways	54%	245	2.98E-112
	RNA polymerase	8%	34	8.15E-31
	Glyoxylate and dicarboxylate metabolism	6%	28	4.39E-25
	Carbon fixation by the Calvin cycle	6%	28	1.88E-24
	Carbon metabolism	6%	28	6.25E-13
BOMI: Upregulated	Protein processing in the ER	26%	49	1.59E-68
	Oxidative phosphorylation	9%	16	1.37E-10
	Spliceosome	6%	12	1.61E-07
	Endocytosis	4%	8	2.15E-04
	Metabolic pathways	16%	29	2.72E-04
	Biosynthesis of unsaturated FAs	2%	3	9.60E-03
RISO-1508 – Upregulated	Protein processing in the ER	37%	47	5.53E-72
	Spliceosome	9%	11	1.34E-07
	Endocytosis	6%	8	3.88E-07
	Ubiquitin-mediated proteolysis	6%	8	6.53E-04

KEGG: Kyoto Encyclopedia of Genes and Genomes. DEGs: Differentially Expressed Genes.

P-values were calculated using KEGG pathway enrichment analysis. Only terms with p<0.05 are shown.

proteolysis (6%, n=8, $P=6.53\times10^{-4}$) was exclusively enriched in RISO-1508, absent from the BOMI upregulated KEGG profile, providing pathway-level confirmation that RISO-1508 preferentially activates protein degradation over refolding under heat stress. Additionally, oxidative phosphorylation (9%, n=16, $P=1.37\times10^{-10}$) was paradoxically enriched among genes upregulated by BOMI, suggesting a compensatory transcriptional upregulation of specific respiratory complex subunits to sustain energy homeostasis—a capacity not observed in RISO-1508.

In BOMI, downregulated DEGs were enriched in oxidative phosphorylation (31%, n=80, $P=6.49\times10^{-82}$), RNA polymerase ($P=3.05\times10^{-33}$), carbon fixation by Calvin cycle ($P=1.03\times10^{-31}$), and photosynthesis (13%, n=33, $P=4.61\times10^{-25}$), reflecting a targeted suppression of plastidic energy metabolism. In RISO-1508, the following pathways were suppressed at dramatically higher gene counts and significance: oxidative phosphorylation (38%, n=171, $P=5.61\times10^{-198}$) and photosynthesis (33%, n=149, $P=3.57\times10^{-191}$), along with metabolic pathways (54%, n=245, $P=2.98\times10^{-112}$), collectively indicating a near-systemic collapse of primary metabolism in the heat-sensitive genotype.

GO Analyses of Downregulated and Upregulated Common/Unmatched Genes

Common downregulated and upregulated genes were identified using the DAVID database to compare the two datasets. According to this analysis, when the gene interaction network in the downregulated genes is examined, as seen in the Venn diagram (Figure 7), BOMI and RISO-1508 show a similar response with 251 common DEGs (Figures 8A and 8B), but 11 genes in BOMI, especially maturase K and photosystem II genes, are reduced, suggesting that the GO functional annotation clusters analysis is impaired in the repair of chloroplasts damaged by heat stress (Figure 9A). However, RISO-1508 clearly has much more serious problems, with only

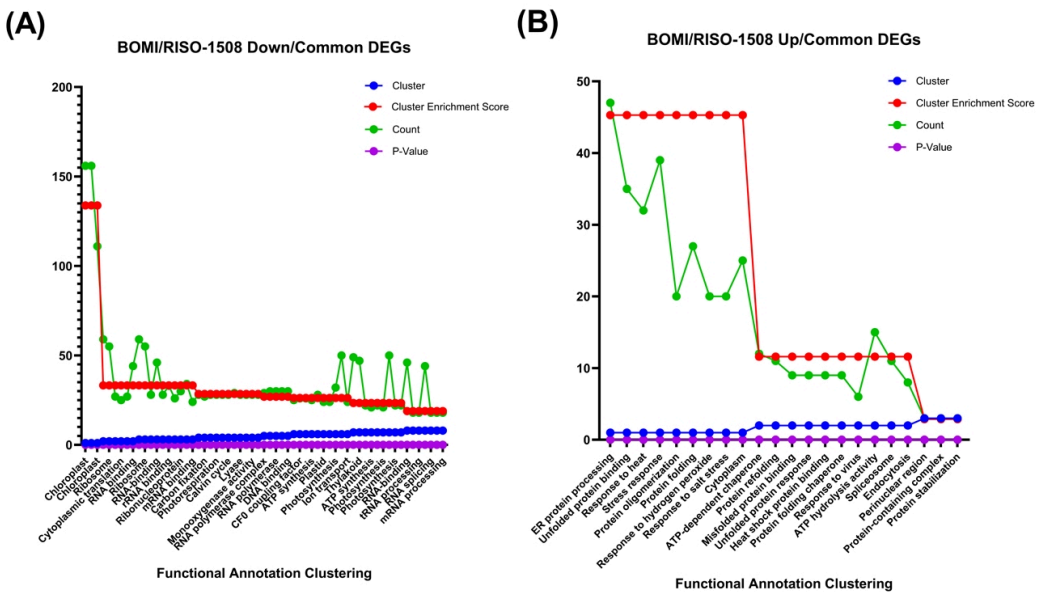

Figure 8. Common DEGs are genes shared between BOMI and RISO-1508. (**A**) Downregulated genes linked to BOMI and RISO-1508, based on log2 (FC) from top DESeq2 results. It depicts shared downregulated genes affected by both in response to heat stress. The DAVID GO analysis (p<0.01) revealed 8 clusters. (**B**) Upregulated genes associated with BOMI and RISO-1508, from DESeq2 lists. This study highlights shared and unique upregulated genes under heat stress. The DAVID GO analysis (p<0.01) identified 3 clusters.

201 genes being downregulated (Figure 9B), unlike BOMI. Here, when log2 (FC) is examined, it is seen in the GO functional annotation clusters analysis that there are serious problems in the Calvin cycle of photosynthesis with the decrease in genes such as *LOC123422470, LOC123423860, LOC123422483,* and *LOC123420794* and in the energy metabolism of photosynthesis with genes such as *LOC123420112, LOC123420286, LOC123420358,* and *LOC123420897.*

According to this GO analysis, when the gene interaction network in the upregulated genes is examined, BOMI and RISO-1508 show a similar response with 90 common genes (Figure 8), as seen in the Venn diagram (Figure 7). However,

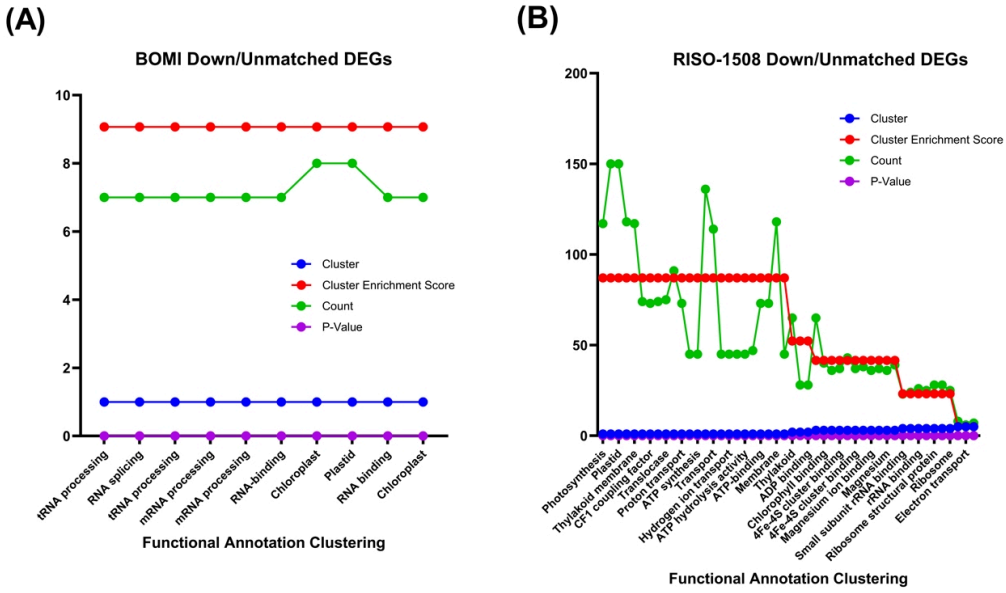

Figure 9. Unmatched DEGs are genes expressed in only one genotype. **(A)** Downregulated genes linked to BOMI, based on log2 (FC) from DESeq2. The results show that 11 unmatched genes are downregulated under heat stress, with only 1 cluster identified (p<0.01). **(B)** Downregulated genes linked to RISO-1508, with 201 unmatched genes downregulated under heat stress and 5 clusters identified (p<0.01).

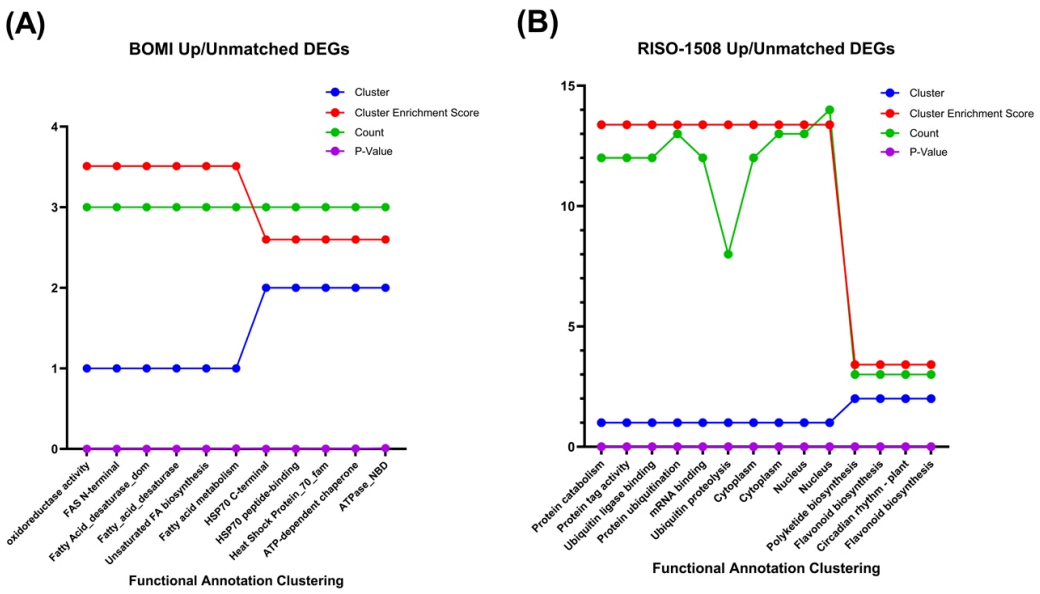

Figure 10. Unmatched DEGs are genes expressed in only one genotype. **(A)** Downregulated genes linked to BOMI, based on log2 (FC) from DESeq2. It shows that BOMI has 95 unmatched and upregulated genes under heat stress, unlike RISO-1508. The DAVID GO analysis (p<0.01) identified 2 clusters. **(B)** The graph shows upregulated genes linked to RISO-1508 from the most expressed DESeq2 results. Unlike BOMI, RISO-1508 has 36 unmatched and upregulated genes under heat stress. The DAVID GO analysis identified 2 clusters.

GO functional annotation cluster analysis revealed that 95 genes were increased in BOMI, unlike RISO-1508 (Figure 10A). Five heat shock proteins were found to be uniquely increased (heat shock 70 kDa protein, BIP5-like-*LOC123399880*, activator of 90 kDa heat shock protein, ATPase homolog-*LOC123407368*, heat shock 70 kDa protein 15-like-*LOC123427066*, heat shock 70 kDa protein, mitochondrial-like-*LOC123450028*, heat stress transcription factor A-2a-like-*LOC123452189*). In addition, a significant difference was observed in fatty acid and energy metabolism (Figure 10A). Under heat stress, the ABA receptor PYL4-like *(LOC123424614)* was significantly upregulated in BOMI compared to RISO-1508, indicating that BOMI exhibits a distinct ABA stress response under heat stress conditions.

GO functional annotation clusters showed that 36 genes were increased in RISO-1508, unlike in BOMI. Specifically, 13 polyubiquitin genes increased, indicating an active response to clear misfolded proteins, affecting growth via auxin and defense. A notable difference in protein processing was found in the endoplasmic reticulum (Figure 10B), which was in contrast with that in BOMI. log2 (FC) analysis revealed that both varieties responded strongly to stress.

DISCUSSION

The effects of heat shock on these genotypes were evaluated using differential gene expression and transcriptomic analyses to identify more resistant barley varieties. Barley stands out as a model species to study the genetic and molecular processes of heat tolerance in the context of global population growth and climate change threats to sustainable crop production.[1] This study investigated the differences in stress responses of wild-type BOMI and its approximately isogenic mutant RISO-1508, which was developed by ethyl methanesulfonate mutagenesis.[26,27] In addition, RISO-1508 exhibited phenotypic differences, such as smaller kernel size, reduced grain yield, decreased starch synthesis, and increased sugar content.[30] These significant phenotypic differences in nutritional and agronomic traits make RISO-1508 a valuable, nutritionally enhanced model species for studying stress responses.

ABA is an important regulator of plant responses to abiotic stresses, such as drought, heat, and salt stress. It also regulates various physiological and developmental processes, such as seed maturation, dormancy, germination, and overall plant growth.[17,36,37] In seed germination experiments, no significant difference in germination dynamics was observed between BOMI and RISO-1508-1508 under control conditions. However, 75 µM ABA treatment almost completely inhibited germination in both lines, consistent with the strong role of ABA in promoting seed dormancy and inhibiting germination. At the seedling developmental stage, 50 µM ABA negatively affected the first leaf growth of both BOMI and RISO-1508-1508. Regardless of ABA exposure, no significant baseline differences in leaf or root length were found between genotypes, indicating that they have a suitable baseline

growth profile to compare their responses under stress. However, significant differences in the severity of ABA-induced inhibition were observed between RISO-1508 and BOMI. Our findings are consistent with those of previous studies that reported similar results in terms of germination time or total viability.[48,49] Both lines exhibited significantly lower ABA-induced root inhibition than the controls, indicating that these barley cultivars possess a specific tolerance or a distinct response mechanism to the effects of ABA on root growth. Changes in ABA signaling may affect the overall stress tolerance of plants by affecting the expression of important transcription factors such as BPBF and ABI5.[43,44] For example, research indicates that suppressing the ABI5 gene in Golden Promise barley, which is cultivated barley, can influence overall stress tolerance, as ABA plays a role in responding to stress.[16] In contrast to these results, our study unexpectedly found that ABA receptor PYL4-like *(LOC123424614)* was significantly higher in BOMI than in RISO-1508 under heat stress. Another study, conducted on a transgenic barley line, supported our findings by showing that the ABA biosynthesis pathway and the key genes for flavonoid and terpene metabolism were upregulated in the transgenic line, demonstrating improved heat and drought tolerance[45] PYL/RCAR proteins are soluble ABA receptors that inhibit PP2C phosphatases upon hormone binding, activating SnRK2 kinases, which phosphorylate ABF/AREB transcription factors to trigger stress responses.[50] The heat-induced rise of PYL4-like *(LOC123424614)* in BOMI likely aids heat tolerance via two mechanisms: First, ABA-mediated stomatal closure limits transpirational water loss under heat stress, supporting cellular water homeostasis.[51] Second, ABA signaling can prime the HSP regulatory network by activating HSFA2 and related heat-shock transcription factors. Zhang et al. (2019)[52] demonstrated that ABA mediates enhanced heat tolerance, specifically through the upregulation of *HsfA2, HSP18,* and *HSP70*. When overexpressed in barley, HSFA2, a key regulator of thermotolerance and heat stress memory, boosts heat tolerance without yield loss.[53,54] The upregulation of five HSPs in BOMI supports activation of the ABA–HSFA2–HSP cascade. The exclusive increase of PYL4-like ABA receptor in BOMI under heat stress indicates higher ABA sensitivity, which may promote thermotolerance through stomatal closure and HSP network priming via SnRK2-AREB pathways. To experimentally discriminate between these pathways, future studies incorporating stomatal conductance measurements and ABA sensitivity assays are warranted. In particular, *ABI5* gene expression plays an important role in ABA-dependent drought responses in barley.[13] Therefore, evaluating these differences in the ABA responses of BOMI and RISO-1508-1508 contributes to a better understanding of the hormonal regulation involved in stress tolerance in these two cultivars.

This study is the first to examine the transcriptomic responses of barley cultivars BOMI and RISO-1508 to heat shock. The observed alignment rate (>50%) is consistent with the ONT cDNA sequencing of large, repeat-rich plant genomes, as the *H. vulgare* Morex v3 genome (~5.3 Gb) is approximately 80% repetitive, inherently limiting, and uniquely mappable reads.[55] ONT-specific artifacts and the presence of non-coding or partially processed transcripts further contribute to this rate, which is considered acceptable and analytically meaningful, as supported by the biologically relevant DEGs identified through DESeq2 analysis. Transcriptomic analyses revealed both shared and cultivar-specific changes in gene expression in BOMI and RISO-1508 under heat stress. BOMI induced higher HSP expression, reflecting a more pronounced chaperone-mediated stress response. A limitation of this study is that post-heat shock recovery was not assessed. Future studies should incorporate recovery time points to determine whether elevated HSP expression in BOMI results in differences in physiological recovery capacity. In the present study, the BOMI heat map clearly shows that genes such as heat shock protein 70 kDa LOC123427066, 16.9 kDa class I heat shock protein 1-like LOC123442570, two types of 26.2 kDa heat shock protein-mitochondrial LOC123409224 and LOC123407668, and 17.5 kDa class II heat shock protein LOC123439499 (Tables 1 and 2) are significantly upregulated (red colour) (Figure 4) in cells under heat shock (BH samples). This finding aligns with the literature.[56–59] HSFs are vital for regulating HSPs in plants, and HSPs are molecular chaperones that stabilize proteins and membranes during heat stress. Plants adapt to moderately high temperatures by rapidly activating heat-sensitive genes, including HSFs and HSPs, thereby gaining heat tolerance. Similar changes in gene expression were observed in the RISO-1508 genotype under heat shock. Upregulation of HSPs: RISO-1508 heat maps showed that HSPs such as heat shock cognate 70 kDa *LOC123440545*, heat shock cognate 70 kDa protein 2 *LOC123402646*, 26.2 kDa heat shock protein, mitochondrial 123408774, 23.2 kDa heat shock protein-like *LOC123430330*, heat stress transcription f *LOC123449300*, and 16.9 kDa class I heat shock protein 1-like *LOC123431205* (Figure 5A) were upregulated (red colour) in RISO-1508 (Figure 5B) heat shock samples (RH samples). These findings are consistent with those of studies conducted on barley. This confirms that RISO-1508 developed a typical defense response to heat shock. Both genotypes exhibited similar primary protective mechanisms by upregulating HSPs under heat stress. In particular, known HSPs, such as 16.9 kDa class 1 heat shock protein and heat shock protein 70 kDa, were observed to

be strongly upregulated under heat stress in both lines. This is consistent with the knowledge that HSFs and HSPs (molecular chaperones that stabilize proteins and membranes) play critical roles in plants' acquisition of acquired heat tolerance in plants.[16,19,20,22,45] The 90 common upregulated genes in the Venn diagram analysis strongly support that the basic defense mechanisms of barley against heat stress are shared. BOMI and RISO-1508 exhibit comparable responses to heat stress. However, BOMI shows greater upregulation of genes, reflecting a more robust stress response. According to the GO functional annotation cluster analysis, 95 genes were increased in BOMI, in contrast to RISO-1508 (Figure 7). Furthermore, five specific HSPs were found to be uniquely elevated in BOMI: heat shock 70 kDa protein BIP5-like *(LOC123399880),* activator of 90 kDa heat shock protein ATPase homolog *(LOC123407368),* heat shock 70 kDa protein 15-like *(LOC123427066),* mitochondrial-like heat shock 70 kDa protein *(LOC123450028),* and heat stress transcription factor A-2a-like *(LOC123452189).* Additionally, notable differences were observed in fatty acid and energy metabolism (Table 1 and Figure 10A. GO functional annotation cluster analysis revealed that the expression of 36 genes was increased in RISO-1508 compared to BOMI. Notably, 13 polyubiquitin genes were upregulated, indicating an active response in clearing misfolded proteins and influencing growth through auxin action and defence. Additionally, significant differences in protein processing were observed in the ER (see Table 2 and Figure 10B). Both varieties exhibited a strong reaction in the stress mechanism. Although observed in different barley varieties, similar results have been reported.[16,43,45,56,60]

In the BOMI Z-score map, several genes, including maturase K *LOC123420950,* chaperone protein ClpB2-chloroplastic *LOC123450068,* two NAD(P)H-quinone oxidoreductase subunits *LOC123418891/LOC12343585,* 30S ribosomal protein S7-chloroplastic *LOC22102,* and photosystem I assembly protein Ycf3 *LOC123420115*, were observed to be downregulated (indicated by blue) in BOMI (Figure 4) heat shock samples in the present study. Although these genes are not referenced in barley literature, similar expression patterns have been reported in plants such as *Arabidopsis rosettes, Tetraena propinqua*, and rice.[61–63] This suggests that basic metabolic processes such as photosynthetic activity or protein synthesis may be suppressed under stress. Environmental changes may disrupt crop plant proteomic and metabolomic pathways. In the RISO-1508 z-score map, many genes, particularly in the upper region, were significantly downregulated (indicated by blue) under heat shock. This included two types of ATP synthase subunit beta-chloroplastic *(LOC123419870/LOC123450068),* photosystem I assembly protein Ycf3 *(LOC123423438),* photosystem I P700-chloroplastic *(LOC123420212),* ribosome-binding factor PSRP1-chloroplastic *(LOC123399637),* petB cytochrome b6 *(HvsvCp053),* 30S ribosomal protein S7-chloroplastic *(LOC123423805),* and two types of NAD(P)H-quinone oxidoreductase subunit L *(LOC123418534/LOC123420364).* In addition, photosynthesis-related genes, such as ribulose bisphosphate carboxylase *(LOC123419585),* were downregulated (Figure 5). Similar patterns were observed in *N. tabacum*, barley, and its CL3 mutant.[64–68] This may indicate that RISO-1508 may experience a more pronounced suppression in photosynthetic capacity or protein synthesis processes under heat stress. Genes involved in the photosynthetic process, such as ATP synthase subunit beta-chloroplastic, Photosystem I, 30S ribosomal protein S7-chloroplastic, and NAD(P)H-quinone oxidoreductase, were generally downregulated under heat stress in both genotypes. This indicates that heat stress impairs the photosynthetic efficiency of plants and that plants respond by adjusting their metabolic activity to mitigate this stress. It is also consistent with the general principle that environmental changes disrupt the proteomic and metabolomic pathways of crop plants.[10,11] When heat maps are examined, it is clear that both genotypes show similar primary responses in upregulating HSP genes in response to heat. However, when z-score maps are considered, downregulation of photosynthetic and ribosomal genes, in particular, is more widespread and stronger (darker blue) in the RISO-1508 genotype than in the BOMI genotype. In particular, many genes related to photosynthesis and protein synthesis (Table 7), such as ATP synthase subunit beta (chloroplastic), photosystem I assembly protein Ycf3, 30S ribosomal protein S7 (chloroplastic), and ribulose biphosphate carboxylase, exhibited more pronounced suppression in RISO-1508 than in BOMI. The lys3a mutation or the general physiological state of RISO-1508 differentially affects the regulation of fundamental processes, such as energy metabolism and protein synthesis, under heat stress. The direct link between the lys3a mutation and heat tolerance is not well established. However, genetic and phenotypic differences likely impact physiological and molecular responses to heat stress. BOMI and RISO-1508 share a similar response with 251 common genes, but RISO-1508 faces more severe issues, with only 201 downregulated genes compared with BOMI. Similar results were observed in WT barley, demonstrating fundamental metabolic processes such as carbohydrate metabolism, the citric acid cycle, amino acid metabolism, and secondary metabolism.[69] Key genes involved in chloroplast repair, such as maturase K and photosystem II genes, are reduced, indicating impaired recovery from heat stress. Additionally, significant problems in the Calvin cycle and photosynthesis energy metabolism are observed

in RISO-1508 due to decreased expression of several critical genes.

Indeed, changes in ABA signaling can shape the general stress tolerance of plants by affecting the expression of important transcription factors such as BPBF and ABI5.[1,13,44] The different gene expression patterns observed in the heat maps may reflect the indirect effects of genotypic variations on the mechanisms of heat stress adaptation. In this context, the RISO-1508-1508 mutant appears to redirect its energy and resources toward the stress response by suppressing photosynthetic and basic metabolic processes more than the BOMI under heat stress.

RISO-1508 had more genes downregulated under heat stress than BOMI (452 vs. 262 genes), with 251 common downregulated genes indicating shared suppression mechanisms. However, RISO-1508 also contained 201 unique downregulated genes, reflecting a broader transcriptional response to heat stress. In contrast, BOMI upregulated more genes than RISO-1508 (185 vs. 126), with 90 common upregulated genes, highlighting shared defense mechanisms against heat stress, whereas BOMI showed greater responsiveness. Plants have a complex central control system that manages stress and development; fully understanding this system is key to making agricultural products more resistant to heat (thermotolerance).[70] Therefore, studies that have found similar results against heat stress have gained importance today. The link between the lys3a mutation and heat tolerance is not well defined, but genetic and phenotypic differences in RISO-1508—such as variations in prolamin, lysine, starch, sugar content, seed size, and yield —likely affect physiological responses to heat stress.[1,30,35] The pronounced downregulation of photosynthetic genes in RISO-1508 indicates thermal suppression and a specific metabolic vulnerability related to the lys3a mutation. The modified carbon/nitrogen flux in this mutant, marked by reduced starch synthesis and increased free sugars, may compromise photosynthetic gene expression during energetic stress. Future research using chlorophyll fluorescence and metabolic flux measurements is crucial for understanding the effects of the lys3a mutation, as gene expression variations in heat maps may reflect indirect impacts on heat stress adaptation.

CONCLUSION

Barley *(H. vulgare L.)* is a valuable cereal grain that ranks fourth among the most important crops produced worldwide. Owing to its superior resistance to stress conditions, it stands out as a model species for studying the genetic and molecular processes of heat tolerance, especially in the context of global population growth and climate change threats to sustainable crop production. The challenges affecting barley production, such as the reduction of crop lands due to global warming, are examined. This study emphasizes the importance of genetically improving crop varieties with increased heat tolerance and stress resistance to these challenges. Heat stress significantly affects gene expression in barley, causing an increase in stress-related proteins and a decrease in genes involved in photosynthesis and basic metabolism. The differences in gene expression between BOMI and RISO-1508 demonstrate that their distinct genetic and phenotypic traits drive different molecular responses to heat stress. The specific sensitivity of BOMI to ABA and its unique gene regulation under heat stress make it a promising model for exploring heat tolerance mechanisms, especially in a nutritionally enhanced genotype. The genotype-specific transcriptional changes included the exclusive activation of *HSP17.5-CII, HSP26.2-Mit,* and *ClpB1* chaperone genes in the heat-tolerant BOMI and the induction of *CIP8* (an E3 ubiquitin ligase) and *BAG6* (a molecular chaperone regulator) in the heat-sensitive RISO-1508. Chaperone-mediated refolding and ubiquitin-proteasome-dependent protein clearance are the key proteostatic strategies underpinning the different thermotolerance phenotypes of the two genotypes. These results lay a strong foundation for genetic research aimed at creating more resilient barley varieties despite global warming. Future research that focuses on functionally characterizing these differentially expressed genes could help develop genetic strategies to boost the heat tolerance of barley and ensure crop yields during climate challenges.

Ethics Committee Approval: Ethical approval is not required for this study.

Peer Review: Externally peer-reviewed.

Author Contributions: Conception/Design of study : E.U. / C.B.S., Data Acquisition: E.U., Data Analysis/Interpretation : E.U. / C.B.S., Drafting Manuscript: E.U., Critical Revision of Manuscript : E.U., Final Approval and Accountability: E.U. / C.B.S., Technical or Material Support: E.U. / C.B.S., Supervision: E.U. / C.B.S..

Conflict of Interest: Authors declared no conflict of interest.

Financial Disclosure: This research was supported by a grant from the COST Action (European Cooperation in Science and Technology) for the project titled “Reproductive Enhancement of Crop Resilience to Extreme Climate” (RECROP; CA22157). Support was provided for a Short-Term Scientific Mission (STSM) fellowship under the grant number E-COST-GRANT-CA22157-13933fa8. EU conducted its research at the Science Building within the Life and Medical Science facilities at the University of Hertfordshire, England.

Acknowledgements We would also like to sincerely thank the RECROP-CA22157 team for the scholarship that made this study possible, and Action Chair Sotirios Fragkostefanakis, for his helpful guidance.

Authors Details

Esma Ulusoy

[1] Uskudar University, Faculty of Engineering and Natural Sciences, Molecular Biology and Genetics, Istanbul, Türkiye

0000-0001-9925-9562 esma.ulusoy@uskudar.edu.tr

Cristina Barrero Sicilia

[2] University of Hertfordshire, School of Life and Medical Science, Department of Clinical, Pharmaceutical and Biological Science Center for Agriculture, Hatfield, Hertfordshire, United Kingdom

0000-0001-7544-5619

REFERENCES

1 Vinje MA, Simmons CH. Characterization of barley (*Horduem vulgare*) lys3 mutants identifies genes under the regulation of the prolamin-box binding transcription factor and elucidates its role in endosperm promoter methylation during grain development. *Mol Genet Genomics*. 2024;299(1):17. doi:10.1007/s00438-024-02112-x

2 *The State of Agricultural Commodity Markets 2024*. FAO; 2024. doi:10.4060/cd2144en

3 Davies WJ, Bennett MJ. Achieving more crop per drop. *Nat Plants*. 2015;1(8):15118. doi:10.1038/nplants.2015.118

4 Ray DK, Gerber JS, MacDonald GK, West PC. Climate variation explains a third of global crop yield variability. *Nat Commun*. 2015;6(1):5989. doi:10.1038/ncomms6989

5 Challinor AJ, Watson J, Lobell DB, Howden SM, Smith DR, Chhetri N. A meta-analysis of crop yield under climate change and adaptation. *Nat Clim Change*. 2014;4(4):287-291. doi:10.1038/nclimate2153

6 Redden R. Wild relatives for the crop improvement challenges of climate change: The adaptation range of Crops. In: Redden R, Yadav SS, Maxted N, Dulloo ME, Guarino L, Smith P, eds. *Crop Wild Relatives and Climate Change*. 1st ed. Wiley; 2015:61-79. doi:10.1002/9781118854396.ch4

7 Baum M, Von Korff M, Guo P, et al. Molecular approaches and breeding strategies for drought tolerance in barley. In: Varshney RK, Tuberosa R, eds. *Genomics-Assisted Crop Improvement*. Springer Netherlands; 2007:51-79. doi:10.1007/978-1-4020-6297-1_3

8 Rae SJ, Macaulay M, Ramsay L, et al. Molecular barley breeding. *Euphytica*. 2007;158(3):295-303. doi:10.1007/s10681-006-9166-8

9 Khakimov B, Rasmussen MA, Kannangara RM, Jespersen BM, Munck L, Engelsen SB. From metabolome to phenotype: GC-MS metabolomics of developing mutant barley seeds reveals effects of growth, temperature and genotype. *Sci Rep*. 2017;7(1):8195. doi:10.1038/s41598-017-08129-0

10 Fernie AR, Schauer N. Metabolomics-assisted breeding: A viable option for crop improvement? *Trends Genet*. 2009;25(1):39-48. doi:10.1016/j.tig.2008.10.010

11 Ricroch AE, Bergé JB, Kuntz M. Evaluation of genetically engineered crops using transcriptomic, proteomic, and metabolomic profiling techniques. *Plant Physiol*. 2011;155(4):1752-1761. doi:10.1104/pp.111.173609

12 An YQ, Lin L. Transcriptional regulatory programs underlying barley germination and regulatory functions of gibberellin and abscisic acid. *BMC Plant Biol*. 2011;11(1):105. doi:10.1186/1471-2229-11-105

13 Collin A, Daszkowska-Golec A, Kurowska M, Szarejko I. Barley ABI5 (Abscisic Acid INSENSITIVE 5) is involved in abscisic acid-dependent drought response. *Front Plant Sci*. 2020;11:1138. doi:10.3389/fpls.2020.01138

14 Dawson IK, Russell J, Powell W, Steffenson B, Thomas WTB, Waugh R. Barley: A translational model for adaptation to climate change. *New Phytol*. 2015;206(3):913-931. doi:10.1111/nph.13266

15 Guo Q, Li X, Niu L, Jameson PE, Zhou W. Transcription-associated metabolomic adjustments in maize occur during combined drought and cold stress. *Plant Physiol*. 2021;186(1):677-695. doi:10.1093/plphys/kiab050

16 Mahalingam R, Duhan N, Kaundal R, Smertenko A, Nazarov T, Bregitzer P. Heat and drought induced transcriptomic changes in barley varieties with contrasting stress response phenotypes. *Front Plant Sci*. 2022;13:1066421. doi:10.3389/fpls.2022.1066421

17 Wang Y, Chang H, Hu S, et al. Plastid casein kinase 2 knockout reduces abscisic acid (ABA) sensitivity, thermotolerance, and expression of ABA- and heat-stress-responsive nuclear genes. *J Exp Bot*. 2014;65(15):4159-4175. doi:10.1093/jxb/eru190

18 Scharf KD, Berberich T, Ebersberger I, Nover L. The plant heat stress transcription factor (Hsf) family: Structure, function and evolution. *Biochim Biophys Acta BBA-Gene Regul Mech*. 2012;1819(2):104-119. doi:10.1016/j.bbagrm.2011.10.002

19 Wang W, Vinocur B, Shoseyov O, Altman A. Role of plant heat-shock proteins and molecular chaperones in the abiotic stress response. *Trends Plant Sci*. 2004;9(5):244-252. doi:10.1016/j.tplants.2004.03.006

20 Mangelsen E, Kilian J, Harter K, Jansson C, Wanke D, Sundberg E. Transcriptome analysis of high-temperature stress in developing barley caryopses: Early stress responses and effects on storage compound biosynthesis. *Mol Plant*. 2011;4(1):97-115. doi:10.1093/mp/ssq058

21 Mishra SK, Chaudhary C, Baliyan S, et al. Heat-stress-responsive HvHSFA2e gene regulates the heat and drought tolerance in barley through modulation of phytohormone and secondary metabolic pathways. *Plant Cell Rep*. 2024;43(7):172. doi:10.1007/s00299-024-03251-6

22 Xue GP, Sadat S, Drenth J, McIntyre CL. The heat shock factor family from *Triticum aestivum* in response to heat and other major abiotic stresses and their role in regulation of heat shock protein genes. *J Exp Bot*. 2014;65(2):539-557. doi:10.1093/jxb/ert399

23 Bailey-Serres J, Parker JE, Ainsworth EA, Oldroyd GED, Schroeder JI. Genetic strategies for improving crop yields. *Nature*. 2019;575(7781):109-118. doi:10.1038/s41586-019-1679-0

24 Munck L, Karlsson KE, Hagberg A, Eggum BO. Gene for improved nutritional value in barley seed protein. *Science*. 1970;168(3934):985-987. doi:10.1126/science.168.3934.985

25 Doll H, Køie B, Eggum BO. Induced high lysine mutants in barley. *Radiat Bot*. 1974;14(2):73-80. doi:10.1016/S0033-7560(74)90179-3

26 Doll H. Inheritance of the high-lysine character of a barley mutant. *Hereditas*. 1973;74(2):293-294. doi:10.1111/j.1601-5223.1973.tb01131.x

27 Ingversen J, Køie B. Lysine-rich proteins in high-lysine *Hordeum vulgare* grain. *Phytochemistry*. 1973;12(5):1107-1111. doi:10.1016/0031-9422(73)85024-1

28 Karlsson KE. Linkage studies in a gene for high lysine content in Risoe barley mutant 1508. *Barley Genet Newsl*. 1977;7(ref.2):40-43.

29 Tallberg A. Comparison between screening methods for lysine with the use of a barley material with a varying amino acid composition. *Acta Agric Scand*. 1979;30(1):26-32. doi:10.1080/00015128009435693

30 Kreis M, Doll H. Starch and prolamin level in single and double high-lysine barley mutants. *Physiol Plant*. 1980;48(1):139-143. doi:10.1111/j.1399-3054.1980.tb03233.x

31 Hejgaard J, Boisen S. High-lysine proteins in Hiproly barley breeding: Identification, nutritional significance and new screening methods. *Hereditas*. 1980;93(2):311-320. doi:10.1111/j.1601-5223.1980.tb01369.x

32 Kreis M. Primer dependent and independent forms of soluble starch synthetase from developing barley endosperms. *Planta*. 1980;148(4):412-416. doi:10.1007/BF00388131

33 Batterham ES. Availability and utilization of amino acids for growing pigs. *Nutr Res Rev*. 1992;5(1):1-18. doi:10.1079/NRR19920004

34 Bose U, Juhász A, Yu R, et al. Proteome and nutritional shifts observed in hordein double-mutant barley lines. *Front Plant Sci*. 2021;12:718504. doi:10.3389/fpls.2021.718504

35 Mena M, Cejudo FJ, Isabel-Lamoneda I, Carbonero P. A Role for the DOF transcription factor BPBF in the regulation of gibberellin-responsive genes in *barley aleurone. Plant Physiol*. 2002;130(1):111-119. doi:10.1104/pp.005561

36 Isabel-LaMoneda I, Diaz I, Martinez M, Mena M, Carbonero P. SAD: A new DOF protein from barley that activates transcription of a cathepsin B-like thiol protease gene in the aleurone of germinating seeds. *Plant J*. 2003;33(2):329-340. doi:10.1046/j.1365-313X.2003.01628.x

37 Yoshida T, Fujita Y, Sayama H, et al. AREB1, AREB2, and ABF3 are master transcription factors that cooperatively regulate ABRE-dependent ABA signaling involved in drought stress tolerance and require ABA for full activation. *Plant J*. 2010;61(4):672-685. doi:10.1111/j.1365-313X.2009.04092.x

38 Nakashima K, Yamaguchi-Shinozaki K. ABA signaling in stress-response and seed development. *Plant Cell Rep*. 2013;32(7):959-970. doi:10.1007/s00299-013-1418-1

39 Yao C, Zhang F, Sun X, et al. Effects of s-abscisic acid (S-ABA) on seed germination, seedling growth, and Asr1 gene expression under drought stress in maize. *J Plant Growth Regul*. 2019;38(4):1300-1313. doi:10.1007/s00344-019-09934-9

40 Finkelstein RR, Gampala SSL, Rock CD. Abscisic acid signaling in seeds and seedlings. *Plant Cell*. 2002;14(suppl 1):S15-S45. doi:10.1105/tpc.010441

41 Fujita Y, Fujita M, Shinozaki K, Yamaguchi-Shinozaki K. ABA-mediated transcriptional regulation in response to osmotic stress in plants. *J Plant Res*. 2011;124(4):509-525. doi:10.1007/s10265-011-0412-3

42 Penfield S. Temperature perception and signal transduction in plants. *New Phytol*. 2008;179(3):615-628. doi:10.1111/j.1469-8137.2008.02478.x

43 Hu Y, Chen X, Shen X. Regulatory network established by transcription factors transmits drought stress signals in plants. *Stress Biol*. 2022;2(1):26. doi:10.1007/s44154-022-00048-z

44 Moreno-Risueno MÁ, Díaz I, Carrillo L, Fuentes R, Carbonero P. The HvDOF19 transcription factor mediates the abscisic acid-dependent repression of hydrolase genes in germinating barley aleurone. *Plant J*. 2007;51(3):352-365. doi:10.1111/j.1365-313X.2007.03146.x

45 Mishra SK, Chaudhary C, Baliyan S, et al. Heat-stress-responsive HvHSFA2e gene regulates the heat and drought tolerance in barley through modulation of phytohormone and secondary metabolic pathways. *Plant Cell Rep*. 2024;43(7):172. doi:10.1007/s00299-024-03251-6

46 Ashburner M, Ball CA, Blake JA, et al. Gene Ontology: Tool for the unification of biology. *Nat Genet*. 2000;25(1):25-29. doi:10.1038/75556

47 Kanehisa M. KEGG: Kyoto Encyclopedia of Genes and Genomes. *Nucleic Acids Res*. 2000;28(1):27-30. doi:10.1093/nar/28.1.27

48 Cook F, Hughes A, Nibau C, et al. Barley lys3 mutants are unique amongst shrunken-endosperm mutants in having abnormally large embryos. *J Cereal Sci*. 2018;82:16-24. doi:10.1016/j.jcs.2018.04.013

49 Howard TP, Fahy B, Craggs A, et al. Barley mutants with low rates of endosperm starch synthesis have low grain dormancy and high susceptibility to preharvest sprouting. *New Phytol*. 2012;194(1):158-167. doi:10.1111/j.1469-8137.2011.04040.x

50 Fidler J, Graska J, Gietler M, et al. PYR/PYL/RCAR receptors play a vital role in the abscisic-acid-dependent responses of plants to external or internal stimuli. *Cells*. 2022;11(8):1352. doi:10.3390/cells11081352

51 Bharath P, Gahir S, Raghavendra AS. Abscisic acid-induced stomatal closure: An important component of plant defense against abiotic and biotic stress. *Front Plant Sci*. 2021;12:615114. doi:10.3389/fpls.2021.615114

52 Zhang X, Wang X, Zhuang L, Gao Y, Huang B. Abscisic acid mediation of drought priming-enhanced heat tolerance in tall fescue (*Festuca arundinacea*) and *Arabidopsis*. *Physiol Plant*. 2019;167(4):488-501. doi:10.1111/ppl.12975

53 Charng Y yung, Liu H chin, Liu N yu, et al. A Heat-inducible transcription factor, HsfA2, is required for extension of acquired thermotolerance in *Arabidopsis*. *Plant Physiol*. 2007;143(1):251-262. doi:10.1104/pp.106.091322

54 Pratx L, Dakhiya Y, Nissen R, et al. Conserved heat shock factors HvHSFA2 and HvHSFA3 control barley heat stress memory through diverged mechanisms. *Nat Commun*. 2025;16(1):10411. doi:10.1038/s41467-025-66651-6

55 Mascher M, Gundlach H, Himmelbach A, et al. A chromosome conformation capture ordered sequence of the barley genome. *Nature*. 2017;544(7651):427-433. doi:10.1038/nature22043

56 Landi S, Capasso G, Ben Azaiez FE, et al. Different roles of heat shock proteins (70 kDa) During abiotic stresses in barley (*Hordeum vulgare*) genotypes. *Plants*. 2019;8(8):248. doi:10.3390/plants8080248

57 Marmiroli N, Pavesi A, Cola GD, et al. Identification, characterization, and analysis of cDNA and genomic sequences encoding two different small heat shock proteins in *Hordeum vulgare*. *Genome*. 1993;36(6):1111-1118. doi:10.1139/g93-148

58 Pandey B, Kaur A, Gupta OP, Sharma I, Sharma P. Identification of HSP20 gene family in wheat and barley and their differential expression profiling under heat stress. *Appl Biochem Biotechnol*. 2015;175(5):2427-2446. doi:10.1007/s12010-014-1420-2

59 Süle A, Vanrobaeys F, Hajós G, Van Beeumen J, Devreese B. Proteomic analysis of small heat shock protein isoforms in barley shoots. *Phytochemistry*. 2004;65(12):1853-1863. doi:10.1016/j.phytochem.2004.03.030

60 Chaudhary R, Baranwal VK, Kumar R, Sircar D, Chauhan H. Genome-wide identification and expression analysis of Hsp70, Hsp90, and Hsp100 heat shock protein genes in barley under stress conditions and reproductive development. *Funct Integr Genomics*. 2019;19(6):1007-1022. doi:10.1007/s10142-019-00695-y

61 Alafari HA, Abd-Elgawad ME. Differential expression gene/protein contribute to heat stress-responsive in *Tetraena propinqua* in Saudi Arabia. *Saudi J Biol Sci*. 2021;28(9):5017-5027. doi:10.1016/j.sjbs.2021.05.016

62 Essemine J, Qu M, Mi H, Zhu XG. Response of chloroplast NAD(P)H dehydrogenase-mediated cyclic electron flow to a shortage or lack in ferredoxin-quinone oxidoreductase-dependent pathway in rice following short-term heat stress. *Front Plant Sci*. 2016;7. doi:10.3389/fpls.2016.00383

63 Yang S, Fang G, Ruan B, et al. Identification of thermo-sensitive chloroplast development gene TSCD5 required for rice chloroplast development under high temperature. *Agriculture*. 2023;13(3):563. doi:10.3390/agriculture13030563

64 Trösch R, Ries F, Westrich LD, et al. Fast and global reorganization of the chloroplast protein biogenesis network during heat acclimation. *Plant Cell*. 2022;34(3):1075-1099. doi:10.1093/plcell/koab317

65 Zubo YaO, Lysenko EA, Aleinikova AYu, Kusnetsov VV, Pshibytko NL. Changes in the transcriptional activity of barley plastome genes under heat shock. *Russ J Plant Physiol*. 2008;55(3):293-300. doi:10.1134/S1021443708030011

66 Danilova MN, Kudryakova NV, Andreeva AA, Doroshenko AS, Pojidaeva ES, Kusnetsov VV. Differential impact of heat stress on the expression of chloroplast-encoded genes. *Plant Physiol Biochem*. 2018;129:90-100. doi:10.1016/j.plaphy.2018.05.023

67 Landau AM, Lokstein H, Scheller HV, Lainez V, Maldonado S, Prina AR. A cytoplasmically inherited barley mutant is defective in photosystem assembly due to a temperature-sensitive defect in *ycf3* splicing. *Plant Physiol*. 2009;151(4):1802-1811. doi:10.1104/pp.109.147843

68 Paul P, Mesihovic A, Chaturvedi P, et al. Structural and functional heat stress responses of chloroplasts of *Arabidopsis thaliana*. *Genes*. 2020;11(6):650. doi:10.3390/genes11060650

69 Chaudhary R, Baliyan S, Sirohi P, et al. Overexpression of barley heat stress transcription factor HvHsfA6a provide thermotolerance by thermopriming. *Mol Biol*. Preprint posted online March 8, 2024. doi:10.1101/2024.03.06.583688

70 Fragkostefanakis S, Röth S, Schleiff E, Scharf K. Prospects of engineering thermotolerance in crops through modulation of heat stress transcription factor and heat shock protein networks. *Plant Cell Environ*. 2015;38(9):1881-1895. doi:10.1111/pce.12396